

Contents lists available at ScienceDirect

Energy

journal homepage: www.elsevier.com/locate/energy





Regulation of reheating temperatures for sCO₂ coal-fired power plant to improve the peak regulation depth

Haonan Zheng ^a, Jinliang Xu ^{a,b,*}, Jian Xie ^{a,b}, Guanglin Liu ^{a,b}

- a Beijing Key Laboratory of Multiphase Flow and Heat Transfer for Low Grade Energy Utilization, North China Electric Power University, Beijing, 102206, China
- b Key Laboratory of Power Station Energy Transfer Conversion and System (North China Electric Power University), Ministry of Education, Beijing, 102206, China

ARTICLE INFO

Handling editor: L Luo

Keywords: sCO₂ cycle Reheating temperature Radiation-convection-reheater Flue gas recirculation Burner angle adjustment Partial load operation

ABSTRACT

Unstable renewable energies can be stabilized by the partial-load-operation (PLO) of supercritical carbon dioxide (sCO_2) coal-fired power plant, under which the reheating temperature deviates from the rated value to deteriorate the efficiency and safety. Challenge exists on the varied heat absorption ratio of the reheater under PLO conditions. We break through the limitation of the reheater arranged in the convection region only for watersteam boiler, but propose a hybrid radiation-convection-reheater (RCRH) for sCO_2 boiler to stabilize the reheating temperature. Three methods including RCRH, flue gas recirculation (FGR) and burner angle adjustment (BAA) are compared, by establishing a partial load model. Our results show that without regulation, the reheating temperature decreases by 32 K at 20 % load, which is not acceptable. FGR and BAA mitigate the reheating temperature deviation to 23 K and 22 K respectively at 20 % load. To satisfy the criterion of 10 K temperature deviation, both FGR and BAA cover the load ratio range of (45–100) %, indicating not effectiveness of these methods. RCRH mitigates the reheating temperature deviation to (1 \sim 2.5) K covering a wide load ratio range of (20–100) %, indicating a large peak regulation depth of 80 % rated power. The proposed RCRH ensures the sCO_2 power plant to operate at an ultra-low load ratio, which is beneficial to balance unstable renewable energies.

1. Introduction

To reduce the carbon dioxide emission, the usage ratio of renewable energies such as solar energy and wind energy continuously increases [1]. A distinct disadvantage of these energies is the unstable nature, inducing the difficulty in balancing the demand side and the supply side of electricity [2]. Energy storage is helpful to balance the user side and the supply side, supplying low-medium capacity (<1 GWh), with the duration time usually being shorter than 4 h [3]. The renewable energies are strongly dependent on weather conditions. When renewable energies are not available for a long time such as one week, it seriously influences the social life to challenge the energy safety.

To overcome the above issue, fossil energy can be partially used to fill the gap of the demand and the supply, which is important especially before ultra-large-scale energy storage technologies are available [4]. For thermal-power conversion using fossil energies, the water-steam Rankine cycle is mature and widely applied in commercial market [5]. Due to large thermal inertia of the power plant, the response of the

Rankine cycle is low with respect to load variations [6]. Alternatively, supercritical carbon dioxide (sCO_2) cycle uses CO_2 to convert thermal energy into power. Due to the gas-like CO_2 fluid in the system and the compact design of the system, the sCO_2 cycle has faster response as load ratio changes, compared with the water-steam Rankine cycle [7]. Hence, the present paper focusses on the sCO_2 cycle under partial-load-operations (PLO).

In 2013, the sCO₂ cycle was first applied to a coal-fired power generation system by Electricity de France (EDF) [8]. Subsequently, sCO₂ coal-fired power generation systems began to be widely studied in various countries. In China, sufficient studies have been performed for sCO₂ coal fired power plant, including cycle analysis and optimization [9–11], component development [12–14], and system demonstration [15,16]. In addition, the 'sCO₂-Flex H2020' project was launched in Europe to study coal-fired power generation systems at partial loads and propose corresponding strategies [17,18]. National Energy Technology Laboratory (NETL) in USA studied the dynamic characteristics of fossil fuel sCO₂ power generation system and concluded that it has a variable

E-mail address: xjl@ncepu.edu.cn (J. Xu).

^{*} Corresponding author. Beijing Key Laboratory of Multiphase Flow and Heat Transfer for Low Grade Energy Utilization, North China Electric Power University, Beijing, 102206, China.

load rate of 7.5%Pe/min [19].

Because the cycle should be coupled with the sCO_2 boiler, two major problems should be solved. Firstly, flue gas temperatures of the boiler have a wide range from $120\,^{\circ}\text{C}$ to $1500\,^{\circ}\text{C}$, extraction of the flue gas energies over the entire temperature range becomes a challenge [10]. To solve this issue, the hybrid top-bottom cycle is proposed to extract the flue gas energies in two different temperature zones respectively [20]. Further, a overlap temperature zone is set, whose heat is absorbed not only by the top cycle, but also by the bottom cycle, called the overlap energy principle [21]. Secondly, the flow rate of the sCO_2 cycle is several times of that of the water-steam Rankine cycle, generating unacceptable pressure drops in the sCO_2 boiler [10]. The proposed partial flow mode decouples a heater into two parallel units, each having the half flow rate [22]. Thus, the pressure drop of the sCO_2 boiler is decreased to a similar level of the water-steam Rankine cycle [15].

Many studies are related to the efficiency improvement [9-11,15, 16]. Wang et al. [15] explored the roadmap to reach the efficiency limit for sCO2 coal fired power plant. Recompression cycle (RC) is widely applied for sCO₂ cycles driven by solar energy and nuclear energy. Based on RC, Wang et al. [15] introduced tri-compression cycle (TC), reheating, double-reheating and inter-cooling. Reheating refers to that after the expansion of the working fluid in the first turbine, the working fluid is reheated by the heat source to raise its temperature and then re-expands in the second turbine to increase the power output. Reheating increases the average heat absorption temperature thus the efficiency increases. We note that reheating is widely applied to increase the efficiency for the water-steam Rankine cycle [23]. Wang et al. [15] found that among various techniques, reheating has the largest contribution to the efficiency improvement for sCO₂ power plant. Thus, sCO₂ coal-fired power generation systems are usually added reheat process to ensure the high efficiency of the system.

At the rated load, the reheating temperature of the working fluid usually equals to that for the primary vapor temperature entering the first turbine [10]. However, this criterion may be broken under PLO conditions. Based on the lessons learned from the water-steam Rankine cycle, the boiler includes the radiation heater in high temperature region located in the furnace, and the convection heater in moderate-low temperature region located in the horizontal flue or the tail flue [24, 25]. The former governs the primary vapor temperature but the latter governs the reheating temperature. Once the load ratio decreases, both the coal consumption rate and the flow rate of water decrease. The flame temperature may not change too much as thermal load changes, but the flow rate of flue gas decreases linearly with respect to load ratios [24]. Correspondingly, the primary vapor temperature is weakly influenced, but the reheating temperature severely decrease [25]. The decrease of reheating temperature not only deteriorates the cycle efficiency, but also threatens the turbine safety [24-26].

For the water-steam boiler, several methods mitigate the reheating temperature. Under PLO conditions, pumping the low temperature flue gas from the tail outlet into the burner increases the cycling flow rate of flue gas, called the flue gas recirculation (FGR) [27]. FGR is believed to reduce the flame temperature, regulating the radiation contribution and the convection contribution to the total load [28]. Due to the enhanced convection contribution, the reheating temperature can be regulated to the rated value [29]. Another method is to dynamically change the burner angle under PLO conditions, called the burner angle adjustment (BAA) [27]. Several layers of burners are arranged along the boiler height direction. At the rated condition, the flame center of these burners coincides with the horizontal plane. As load decreases, the burner angle is changed to deviate from the horizontal plane, regulating the radiation ratio and the convection ratio of the total load. Hence, the reheating temperature can be mitigated [30]. The successful application of this method depends on the smart control of the boiler system [31].

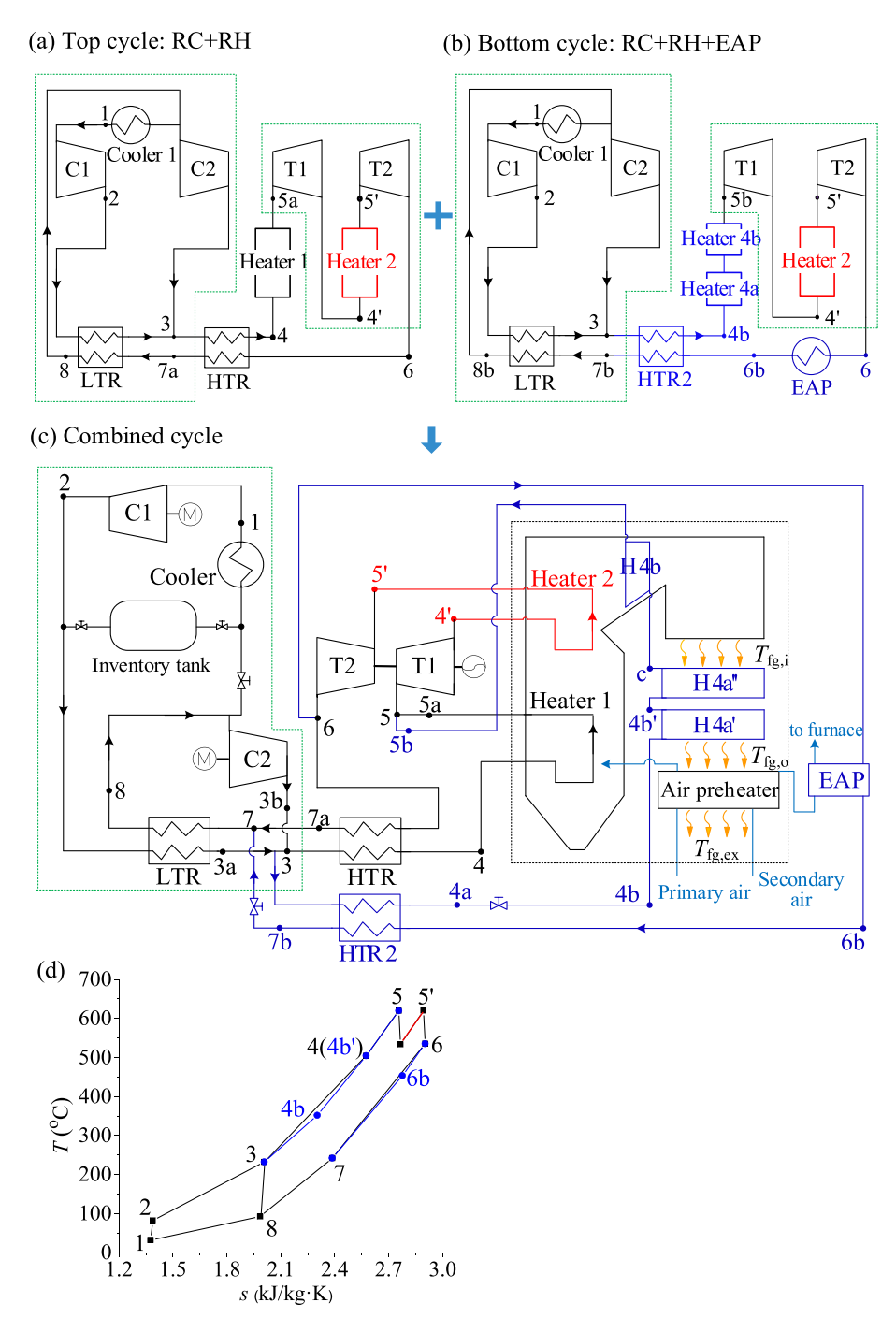
There are some differences between water-steam boiler and sCO_2 boiler. Therefore, it is uncertain whether the strategy described above for water-steam systems is applicable to the sCO_2 system. Firstly, the

 CO_2 is in supercritical state all the time In the sCO $_2$ cycle, so the pressure ratio of system is small, which makes the turbine exhaust temperature higher. Moreover, the heat of the remunerators is $3{\sim}4$ times of the power generation. These make the sCO $_2$ temperature entering the boiler is ${\sim}200~^{\circ}C$ higher than the water entering temperature [15]. Secondly, the CO $_2$ flow rate is ${\sim}8$ times higher than the flow rate of water [14]. Thirdly, the arrangement of sCO $_2$ heaters is different from that of the water-steam boiler. For the former, the modular heaters are applied to address the pressure drop issue [10], but the water-steam boiler uses more integrated heater. The above factors influence the radiation component and the convection component of the heat absorption rate to affect the reheating temperature.

Here, we aim to propose smart methods to control the reheating temperature for sCO_2 coal fired power plant. Three methods are introduced, including the flue gas recirculation (FGR) and the burner angle adjustment (BAA), and the hybrid radiation-convection-reheater (RCRH), among which the FGR and the BAA are borrowed from the water-steam boiler, but the RCRH is newly proposed in this paper. We establish a partial load model to assign the total thermal load of the boiler to various heater modules for sCO_2 boiler under PLO conditions. These heater modules are coupled with the thermodynamics cycle. We conclude that the FGR and the BAA are not suitable for the sCO_2 power plant. It is found that the RCRH successfully regulates the reheating temperature with the load ratios in the range of (20–100)%, corresponding the peak regulation depth of 80 % rated load, which is perfect to balance the unstable renewable energies.

2. The sCO₂ cycle coupling with the sCO₂ boiler

Fig. 1 shows the cycle, which is modified from Ref. [22]. The cycle is designed at the rated capability of 300 MWe. It is a combined cycle, including a top cycle and a bottom cycle. Fig. 1a and b describe the top cycle and the bottom cycle, respectively. The top cycle is a recompression + reheat cycle (RC + RH) and the bottom cycle is a recompression + reheat + external air preheater (RC + RH + EAP) cycle. The two cycles extract flue gas heat in high and medium temperature levels, respectively. Even though the flow rates of sCO2 in the two cycles are different, pressures and temperatures of sCO2 are similar in the two cycles. Hence, the components sharing technique is applied to simplify the system layout [21]. Fig. 1c shows the top-bottom combined cycle constructed by sharing some components of the top cycle and bottom cycle. The components in the green box are the shared components. The black components represent the top cycle, while the blue components represent the bottom cycle. Two turbines of T1 and T2 are included in the cycle, among which T1 is the primary turbine and T2 is the reheating turbine. The cycle contains two compressors of C1 and C2. HTR and HTR2 are the two high-temperature-recuperators, where the former and the latter are used to recover heat for the top cycle and the bottom cycle, respectively. LTR is the low-temperature-recuperator, which is shared by the top cycle and the bottom cycle. The external-air-preheater (EAP) extracts part of the heat from sCO₂ leaving T2. The black dashed box in Fig. 1c is the sCO₂ boiler. Heater 1 drives the top cycle. Heater 2 drives both the top cycle and the bottom cycle. Heater 4a', 4a'' and 4b are the heaters to drive the bottom cycle. In sCO2 boiler, the yellow and light blue lines represent the air flow and the flue gas flow, respectively. The entire flue gas energies are absorbed by the sCO2 cycle and the air-preheater (AP), satisfying the cascade energy utilization principle [20]. The primary and secondary air is first sent to the AP to absorb the heat from the flue gas. After that, the primary air is sent to the furnace and the secondary air is sent to the EAP to exchange heat with CO2 before being sent to the furnace chamber. The flue gas passes through the furnace chamber, the horizontal flue and the tail flue in turn to transfer heat to CO₂ or air. Fig. 1d shows T-s diagrams of the system, in the bottom cycle, the heat of EAP is sent to the furnace for heating the CO_2 to $T_{4b'}$, giving equal efficiency to the top and bottom cycles.



 $\textbf{Fig. 1.} \ \, \textbf{The sCO}_2 \ \, \textbf{cycle} \ \, \textbf{coupled} \ \, \textbf{with the boiler heater (a: top cycle; b: bottom cycle; c: Combined cycle; d: T-s diagram for the system)}.$

3. The methods to regulate reheating temperatures

We describe the methods to regulate the reheating temperatures for the water-steam boiler first. Then, we comment on how these methods are adapted to the ${\rm sCO_2}$ boiler. The RCRH method is proposed in the end of this section.

3.1. The FGR and BAA methods to regulate reheating temperatures for water-steam boiler

The regulation of reheating temperature for water-steam boiler is important under PLO conditions [26]. Four methods exist to regulate the reheating temperatures, including the flue gas recirculation (FGR)

method, the burner angle adjustment (BAA) method, the flue gas damp adjustment (FDA), and the spray attemperation (SA) method [27]. Because SA is used under accident condition and it deteriorates the system efficiency, it is omitted here. FDA is suitable for the water-steam boiler but may not be suitable for the sCO $_2$ boiler, hence it is not further discussed here.

We focus on the discussion on FGR and BAA (see Fig. 2). FGR is widely applied in the water-steam boiler [28]. Part flow rate of the flue gas from the tail flue is recycled into the furnace. Because the high temperature flue gas due to coal burning and the low temperature flue gas due to recycling are mixed in the furnace, the flame temperature $T_{\rm flame}$ decreases. Because radiation heat transfer is proportional to $T_{\rm flame}^4$, the decrease of $T_{\rm flame}$ decreases the radiation component of the boiler

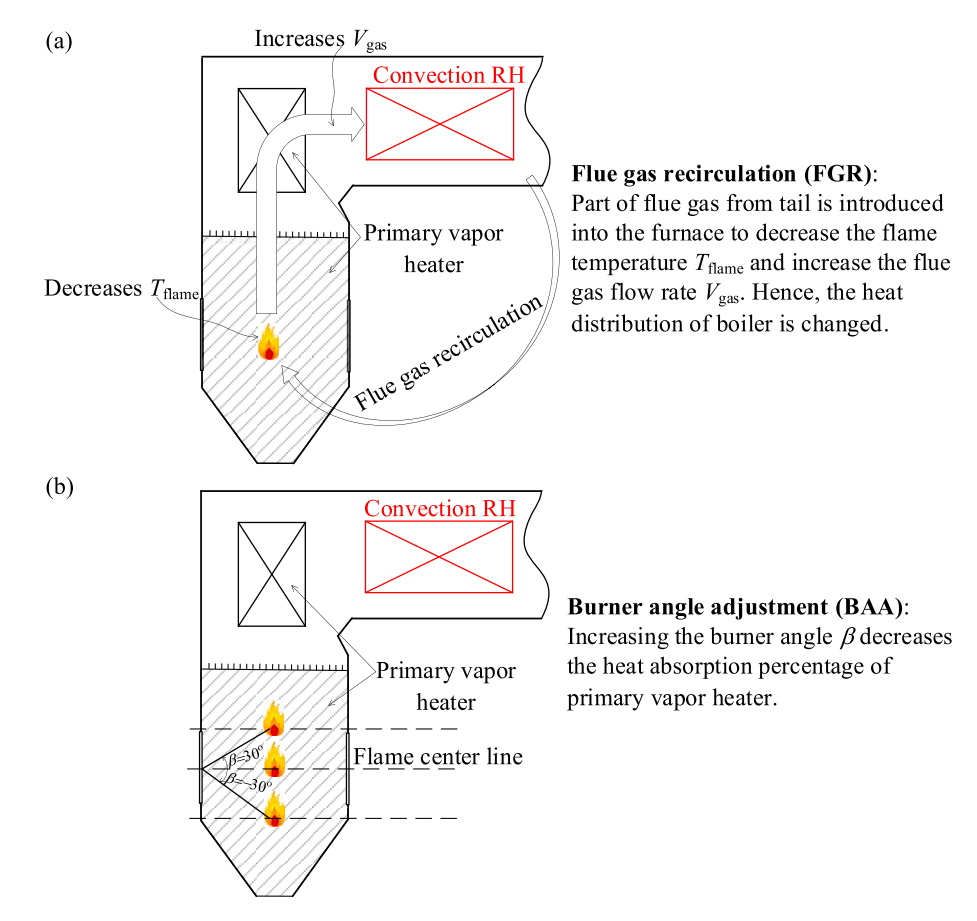


Fig. 2. The regulation of reheating temperature for the water-steam boiler (a: Flue gas recirculation FGR method; b: burner anger adjustment BAA method).

load. Meanwhile, FGR increases the flue gas flow rate, increasing the convection component of the boiler load. Because the reheater is located in the convection region, FGR increases the reheating temperature, which increases by 2.1 K as the recycling ratio of the flue gas increases by 1 % [29]

BAA also controls the reheating temperature [27]. At the rated power, the flame center usually coincides with the horizonal plane. The burner angle β is defined as the deviation of the flame center from the horizontal plane. During partial load operation, the increase of β elevates the flame center height. Hence, the radiation component decreases but the convection component increases [25]. The reheating temperature increases, which increases by 7 K if β increases by 10° [25].

3.2. The FGR and BAA methods to regulate reheating temperatures for sCO_2 boiler

We describe how the methods applied for the water-steam boiler can be adapted to the sCO_2 boiler. A distinct difference of the sCO_2 boiler and the water-steam boiler lies in that the modular heaters should be used to decrease the pressure drops in the boiler [10]. As shown in Fig. 3a, The black dotted line is the outlet of the furnace, which is the dividing line between radiative heat transfer zone and convective heat transfer zone. On the left side of the dotted line, the flue gas transfers heat to the CO_2 by radiative heat transfer, while on the right side of the dotted line, the flue gas transfers heat to the CO_2 by convective heat transfer. The boiler is decoupled into several modules such as Heater 1, Heater 2 and H4a and H4b, in which Heater 1 and H4a and H4b form the main heater to drive the primary turbine T1, and Heater 2 to drive the reheating turbine T2 (see Fig. 1). Due to the partial flow strategy used [22], the Heater 1 consists of two parallel lines, with Part 1 and SH1 as one line and Part 2 and SH2 as the other line, where SH represents

superheater. Each line accounts for the half flow rate to decrease the pressure drops. Similarly, the Heater 2 includes LRH1 and HRH1 as one line, and LRH2 and HRH2 as the other line, where L and H mean low temperature and high temperature respectively, RH means reheater. Hence, the total thermal load of the heater ($Q_{\rm H}$) is decoupled into two components: $Q_{\rm H} = Q_{\rm MH} + Q_{\rm RH}$, where $Q_{\rm MH}$ is the load of main heater and $Q_{\rm RH}$ is the reheating load. The reheater is located in the convection region.

In the boiler, an origin point O for x-y-z axes is usually defined at the center height of the ash hopper to describe the dimensions of boiler. For example, the furnace height is H_b , starting from the original point O to the furnace roof. The heat fluxes on the furnace wall is not uniform in the height direction. A typical non-uniform coefficient of heat flux distribution is plotted in Fig. 3b, which is used to assign the boiler load to various heater modules along the height direction [22]. The non-uniform coefficient of heat flux distribution in Fig. 3b is from the data of steam π -type boiler in Ref. [32]. Which is suit to the pulverized coal and π -type boiler boilers. The dimensions of a sCO₂ boiler and a water-steam boiler is similar. Although the CO2 temperature entering the boiler increases the cooling wall temperature, the heat flux in furnace q is not sensitive to the change of the cooling wall temperature $T_{
m w}$ due to the scale law of $q \sim \left(T_{
m fire}^4 - T_{
m w}^4\right)$, noting the temperature unit of K. For example, assuming a fire temperature $T_{\rm fire}$ of 1600 °C and an increase in cooling wall temperature $T_{\rm w}$ from 600 °C to 700 °C, the heat heat flux q is only 2.7 % in error. Therefore, in the absence of experimental data for sCO2 boiler, it is relatively reasonable to use the water-steam boiler heat flux curve for calculation [22].

Fig. 4 illustrates the sCO₂ boiler design using the modular design. The modules of Part 1, Part 2 and H4b belong to the cooling wall heaters, which are dominated by radiation heat transfer. SH1 and SH2 are the platen heaters. HRH1 and HRH2 are the suspending heaters, LRH1,

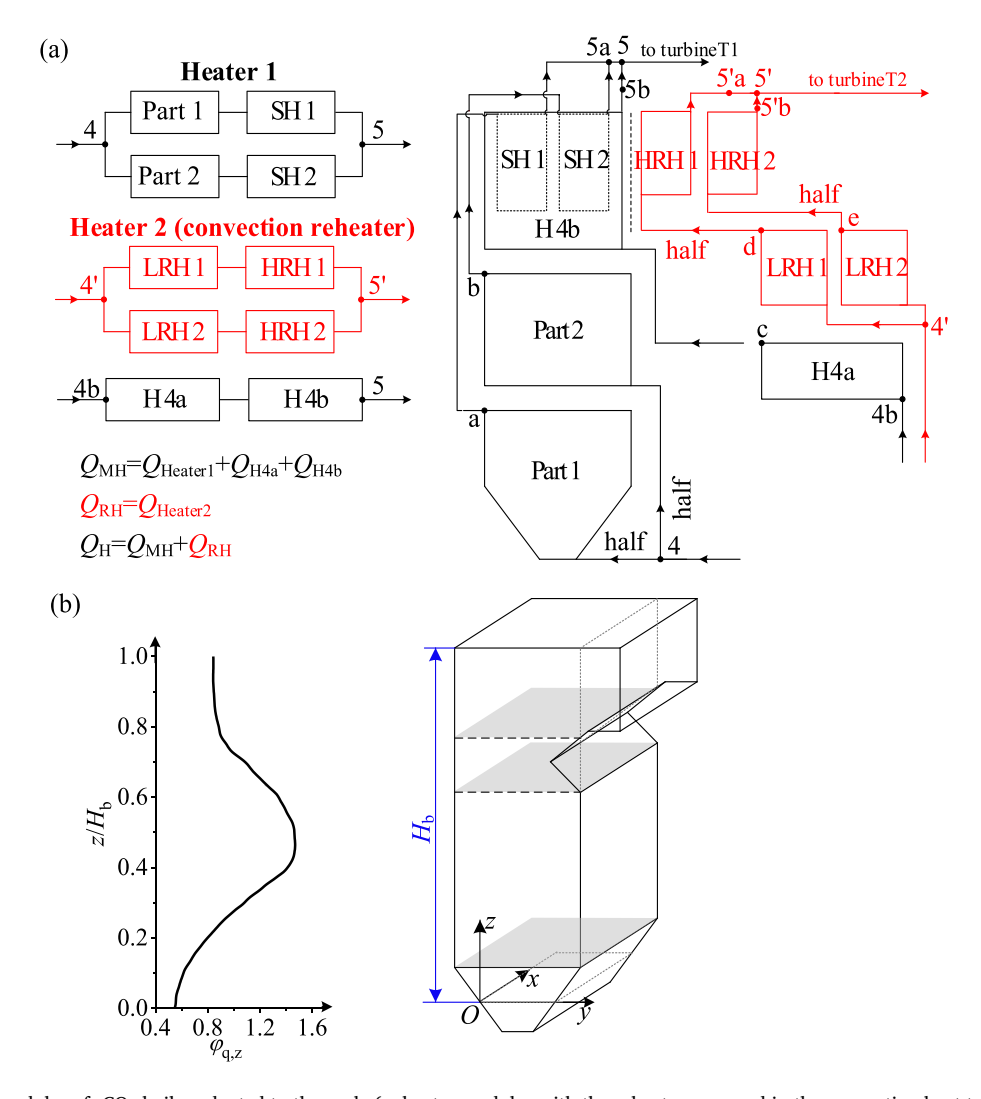


Fig. 3. Various heater modules of sCO₂ boiler adapted to the cycle (a: heater modules with the reheater arranged in the convection heat transfer dominated region and marked by the red color; b: the non-uniform-heat-distribution-coefficient in the boiler height direction).

LRH2 and H4a are the fined-tube-heat-exchangers with sCO₂ flowing in tubes and flue gas flushing fin surfaces. All the reheater modules are dominated by convection heat transfer on the flue gas side, enclosed by the red frame. In the tail flue of boiler, a flue gas extraction port is stetted below H4a, through which part of the low-temperature flue gas is resent to furnace's bottom by a fan (see Fig. 4). r_{FGR} is the volume ratio of recirculated flue gas to total flue gas. $r_{FGR} = 0$ under rated conditions, and its maximum value is 30 % to guarantee stable combustion of coal [24]. By adjusting the power of the fan, r_{FGR} may be modified to achieve the regulation of reheating temperature. Besides, the sCO₂ boiler adopts the corner tangential combustion method, with a total of 6 layers of swing burners arranged at the corners of the furnace. There are 5 layers of separated overfired air (SOFA) nozzles in the upper part of the furnace to ensure the pulverized coal burn out fully. The up-down angle β of the swing burner has an adjustable range of $\pm 30^{\circ}$ [24], and the regulation of reheating temperature may be realized by adjusting β .

3.3. The RCRH method to regulate reheating temperatures for sCO_2 boiler

The above sections indicate that for water-steam boilers, the cooling wall is designed as an integrated component to be dominated by radiation heat transfer. The reheater can only be arranged in the moderate temperature region, which is dominated by convection heat transfer, resulting in the decrease of reheating temperature as boiler load decreases. The FGR and BAA methods are used to compensate the decrease

of reheating temperatures. The effectiveness of the FGR and BAA methods for the sCO₂ boilers should be verified.

The distinct difference of the two boilers lies in that more heater modules shall be used for the sCO₂ boiler to address the pressure drop issue, inspiring us to freely arrange heater modules. This feature generates the hybrid arrangement of the reheater modules, which is shown in Fig. 5a. The black line and red line represent Heater 1 and Heater 2, also known as the main heater and reheater, respectively. The reheater is decoupled into four modules of Part 3, Part 4, RH1 and RH2, among which Part 3 and Part 4 belong to cooling wall type modules which are dominated by radiation heat transfer, RH1 and RH2 are operated in moderate temperature zone which are dominated by convection heat transfer. The reheater becomes a hybrid radiant-convection reheater (RCRH), which is significantly different from Fig. 3a. The arrangement of reheater modules is enclosed by the red frame in Fig. 5b. It is expected that in such a way, the heat absorption ratio of the reheater synchronously varies as load ratio changes to stabilize the reheating temperature, which will be commented further.

4. Numerical methods

According to the parameters listed in Table 1, the sCO₂ coal-fired generation system and components have been designed in the literature [33]. Tables 2 and 3 show the parameters of heater modules in sCO₂ boiler, and the technical parameters of the turbomachinery under rated

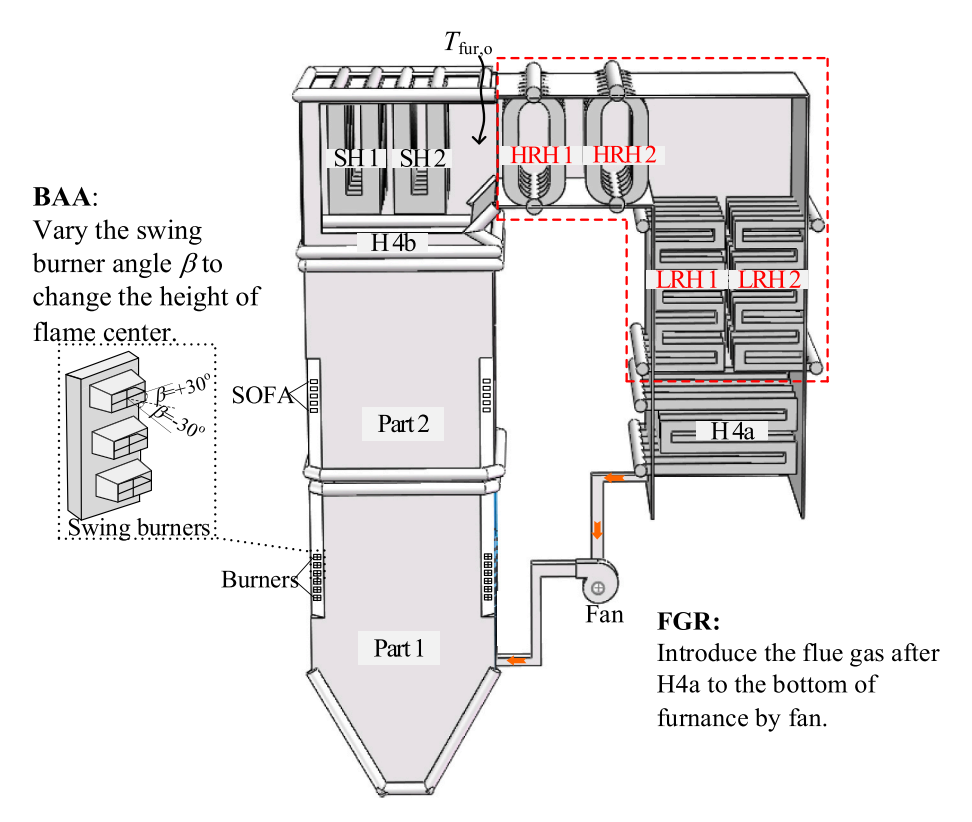


Fig. 4. The FGR and BAA methods adapted to the sCO₂ boiler.

conditions, respectively. These serve as the basis for the partial load study of the system. Table 4 shows the parameters of each state point in the system under design conditions. In this paper, we focus on the partial load model of the sCO_2 coal-fired generation system. The thermal load assignment model, the coupling of the sCO_2 cycle with the components, and the numerical method were described in the following sections.

4.1. The thermal load assigned to various heater modules for sCO₂ boiler

The boiler load calculation at the rated capacity of 300 MWe can be found in Ref. [22]. The load assignment under the partial load operation is paid attention here. Under PLO condition, recording the cycle efficiency as $\eta_{\text{th,PLO}}$ (determined in Section 4.2), the boiler load is

$$Q_{\text{boiler,PLO}} = \frac{\eta_{LD} W_{\text{net,R}}}{\eta_{\text{th,PLO}}} \tag{1}$$

Where $\eta_{\rm LD}$ is the load ratio, which is in the range of (20–100) %, $W_{\rm net,R}$ is the power capacity at the rated condition, which is 300 MWe here. The excess air coefficient α and the air leakage factor $\Delta\alpha$ are [24,34]

$$\begin{cases} \alpha_{\text{PLO}} = \alpha_{\text{R}} & \text{if} \quad \frac{Q_{\text{boiler,PLO}}}{Q_{\text{boiler,R}}} \ge 0.7 \\ \\ \alpha_{\text{PLO}} = \alpha_{\text{R}} + 0.7 - \frac{Q_{\text{boiler,PLO}}}{Q_{\text{boiler,R}}} & \text{if} \quad \frac{Q_{\text{boiler,PLO}}}{Q_{\text{boiler,R}}} < 0.7 \end{cases}$$

$$\Delta \alpha_{\text{PLO}} = \Delta \alpha_{\text{R}} \left(\frac{Q_{\text{boiler,R}}}{Q_{\text{boiler,PLO}}} \right)^{0.5} \tag{3}$$

where Q_{boiler} is the thermal load of the boiler, the subscripts PLO and R refer to the PLO condition and the rated condition, respectively. We note that q_2 is a major contribution for heat loss, which is influenced by α and

 $\Delta \alpha$. The boiler efficiency η_b is

$$\eta_b = 1 - q_2 - q_3 - q_4 - q_5 - q_6 \tag{4}$$

where q_2 , q_3 , q_4 , q_5 and q_6 are heat losses due to exhaust gas, unburned gases loss, unburned carbon loss, radiation, and sensible heat in slag, whose computation can be found in Ref. [22]. The coal consumption

$$m_{\text{coal,PLO}} = \frac{Q_{\text{boiler,PLO}}}{\eta_{\text{b}} Q_{\text{LHV}}} \tag{5}$$

where $Q_{\rm LHV}$ is the lower heating value of the coal, noting that Eq. (5) is valid for both rated condition and PLO condition.

The boiler load includes the radiation component and the convection component. The flue gas temperature at the furnace outlet $T_{\rm fur,o}$ characterizes the interface between the two components, above which is the radiation contribution and below which is the convection contribution. $T_{\rm fur,o}$ is [24].

$$T_{\text{fur,o}} = \frac{T_{\text{flame}}}{1 + M \left(\varepsilon_{\text{fur}}^{\text{syn}} / Bo\right)^{0.6}} \tag{6}$$

where $T_{\rm flame}$ is the fuel combustion temperature, which is related to the ratio of air to the coal. According to Eq. (2), the excess air coefficient α varies with the load, so $T_{\rm flame}$ changes at partial load. M characterizes the flame position, which is [24].

$$M = 0.59 - 0.5(x_{\rm B} + \Delta x) \tag{7}$$

Where x_B is the relative height of the burner, $\Delta x = 0.1$ corresponds to the burner angle adjustment (BAA) of 20°, assuming the linear variation of Δx with respect to BAA. $\varepsilon_{\rm fur}^{\rm syn}$ is the comprehensive blackness of the

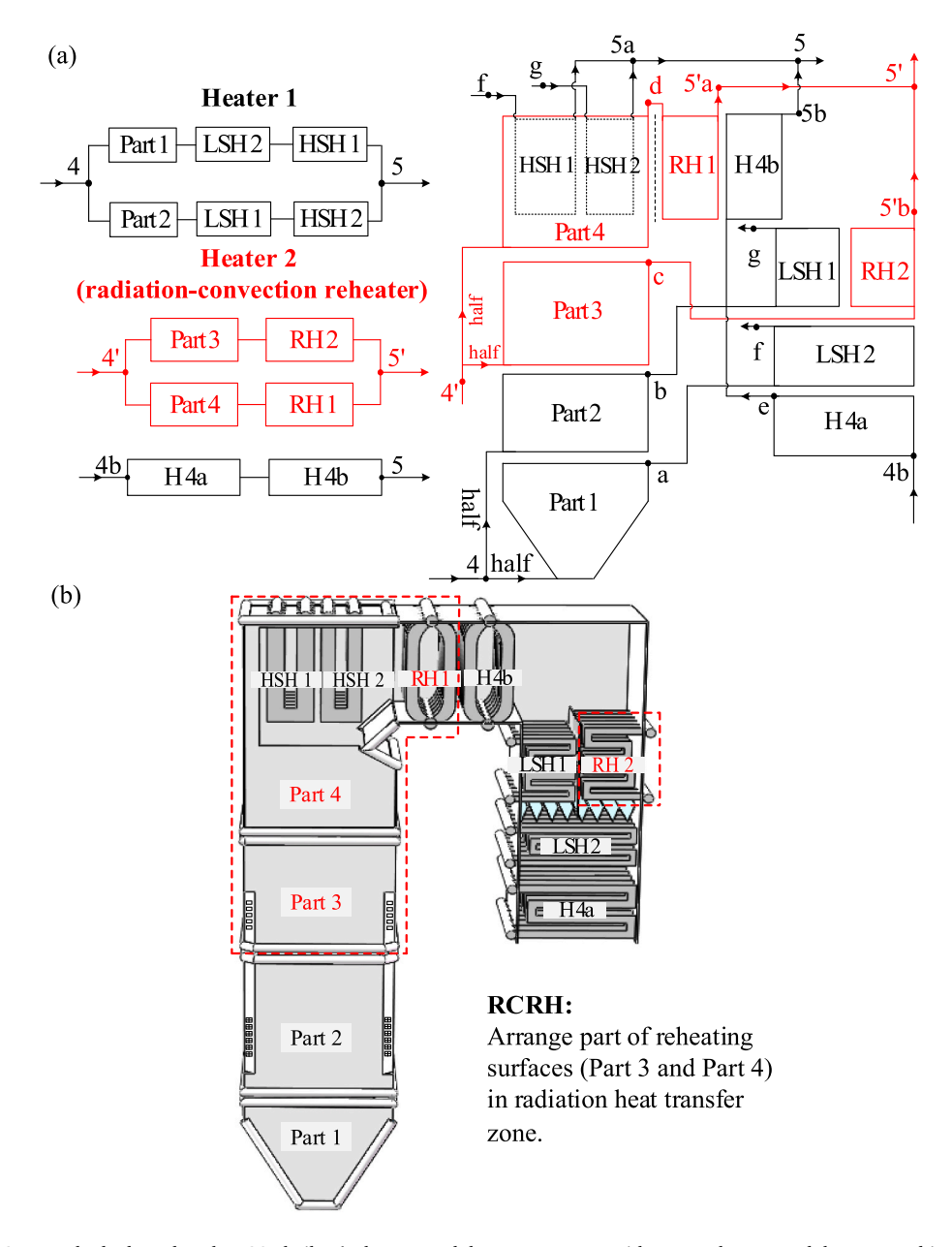


Fig. 5. The proposed RCRH method adapted to the sCO₂ boiler (a: heater modules arrangement, with some reheater modules arranged in the radiation dominated region and the others arranged in the convection dominant region; b: the sCO₂ boiler using RCRH).

burner. Hence, the radiation load is [24]

$$Q_{\text{fur,PLO}} = \phi m_{\text{coal,PLO}} C_{\text{flue,ave}} (T_{\text{flame}} - T_{\text{fur,o}})$$
(8)

Where ϕ is the heat retention coefficient of the boiler, $\phi=1$ - $q_5/(\eta_b+q_5)$, $C_{\rm flue,ave}$ is the specific heat of the flue gas in the burner.

Then, the average radiation heat flux of the burner q_{ave} is

$$q_{\text{ave,PLO}} = \frac{Q_{\text{fur,PLO}}}{A_{\text{b}} + A_{\text{SH}}} \tag{9}$$

where $A_{\rm b}$ and $A_{\rm SH}$ are the surface areas of the cooling walls and the superheater (SH), respectively.

For heater module arrangement such as shown in Fig. 3a, the radiation load assigned to various modules are

$$\begin{cases} Q_{\text{Part1}} = \int_{0}^{z_{1}} q_{ave} \varphi_{q,z} A_{\text{Part 1}} dz \\ Q_{\text{Part2}} = \int_{z_{1}}^{z_{2}} q_{ave} \varphi_{q,z} A_{\text{Part 2}} dz \end{cases}$$

$$\begin{cases} Q_{\text{H4b}} = \int_{z_{2}}^{z_{2}} q_{ave} \varphi_{q,z} A_{\text{H 4b}} dz \\ Q_{\text{SH1}} = \int_{z_{4}}^{H_{b}} q_{ave} \varphi_{q,z} A_{\text{SH 1}} dz \\ Q_{\text{SH2}} = \int_{z_{5}}^{H_{b}} q_{ave} \varphi_{q,z} A_{\text{SH 2}} dz \end{cases}$$

$$(10)$$

Where $\varphi_{q,z}$ is the non-uniform coefficient, which is predicted based on Fig. 3b. For the RCRH shown in Fig. 5, the radiation load assigned to heater modules in the burner are treated similarly to that shown in Eq. (10).

The computation of radiation heaters depends on the flue gas side

Table 1Parameters for the cycle computations and boiler design.

Parameter	Values
Net power (W_{net})	300.0 MW
Turbine inlet temperature (T_5 , T_5)	620.0 °C
Turbine T1 inlet pressure (P ₅)	30.0 MPa
Compressor C1 inlet temperature (T_1)	32.0 °C
Compressor C1 inlet pressure (P_1)	7.6 MPa
Turbines isentropic efficiency ($\eta_{T,s}$)	0.93
Compressors isentropic efficiency ($\eta_{C,s}$)	0.89
Pinch temperature difference in LTR/HTR (ΔT)	10.0 °C
Max pressure drop in LTR/HTR/Cooler (ΔP)	0.2 MPa
Pinch temperature difference in Cooler (ΔT_{Cooler})	5.0 °C
Cooling water temperature (T_{water})	25.0 °C
Exhaust gas temperature ($T_{fg,ex}$)	123.0 °C
Environment temperature (T_0)	20.0 °C
Excess air coefficient (α)	1.2
Primary/Secondary air temperature entering air preheater	31.0 °C
air temperature entering air preheater	23.0 °C
Ratio of primary air flow rate to the total air flow rate	0.19

Table 2Design parameters of heater modules of sCO₂ boiler.

Heat exchange modules	$d_{ m i} imes \delta$ (mm)	d _o (mm).	s ₁ (mm)	s ₂ (mm)	A (m ²)	Heat absorption Q (MW)
Part1	24 × 8	40	56	_	850.1	112.6
Part2	24×8	40	56	_	651.6	112.6
H4b	20×6	32	45	_	242.2	30.0
SH	32×8	48	1350	60	919.5	55.5
HRH	35×5	45	450	60	3227.1	116.2
LRH	48×5.5	59	120	74	14209.0	116.2
H4a	48×5.5	59	120	74	43436.7	63.0
EAP	48×5.5	59	106	74	2253.7	17.8
AP	_	_	_	_	80743.6	80.1

Table 3Technical parameters of turbomachines at design condition.

Items	C1	C2	T1	T2
T _{in} (°C)	32.0	92.5	620.0	620.0
$P_{\rm in}$ (MPa)	7.6	7.8	30.0	15.7
$T_{\rm out}$ (°C)	82.5	232.1	533.7	535.5
P_{out} (MPa)	31.2	31.1	15.8	8.2
m (kg/s)	1467.6	710.2	2177.8	2177.8
η (%)	89.0	89.0	93.0	93.0
N (rpm)	3000	3000	3000	3000
W (MW)	57.2	73.9	217.0	214.2

only. For convection heaters, the load assignment is a coupling of the flue gas side and the CO_2 side. There are several heater modules in the horizontal flue and tail flue, including HRH1, HRH2, LRH1, LRH2 and H4a (see Fig. 3a), and RH1, H4b, LSH1, RH2, LSH2 and H4a (see Fig. 5). These heater modules are calculated consecutively along the flow direction of the flue gas. For any convection heater module, the inlet and outlet flue gas temperatures are recorded as $T_{\mathrm{fg,i}}$ and $T_{\mathrm{fg,o}}$. The heat load for this module $Q_{\mathrm{C,PLO}}$ is

$$Q_{\text{c.PLO}} = \phi m_{\text{coal,PLO}} C_{\text{flue,ave}} \left(T_{\text{fg,i}} - T_{\text{fg,o}} \right) \tag{11}$$

On the other hand, $Q_{c,PLO}$ is predicted based on the heat transfer principle as

$$Q_{c,PLO} = KA_c \Delta T \tag{12}$$

where A_c is the heat transfer area for the heater module, ΔT is the logarithmic mean temperature difference between the flue gas and the sCO₂. K is the heat transfer coefficient [24].

Table 4Main parameters of sCO₂ cycle at design condition.

State points	Pressure/MPa	Temperature/°C	Enthalpy/kJ/kg
1	7.6	32.0	315.1
2	31.2	82.5	352.4
3a	31.1	232.1	608.4
3b	31.1	232.1	608.4
3	31.1	232.1	608.4
4	31.0	504.8	971.5
4a	30.9	352.7	774.4
4b	30.1	352.0	774.4
5	30.0	620.0	1118.2
5a	30.0	620.0	1118.2
5b	30.0	620.0	1118.2
4'	15.8	533.7	1019.5
5'	15.7	620.0	1121.8
6	8.2	535.5	1027.1
6b	8.2	453.2	927.8
7	8.0	242.1	680.3
7a	8.0	242.1	680.3
7b	8.0	242.1	680.3
8	7.8	92.5	508.3

$$K = \psi \frac{1}{\xi \frac{1}{a_{f_{E}}} + \frac{1}{a_{f}}} \tag{13}$$

where ξ is the correction factor, $\alpha_{\rm fg}$ and $\alpha_{\rm f}$ are the heat transfer coefficients in the flue gas side and the sCO₂ side, respectively. The determination of $Q_{\rm c}$ needs the iterative computation, which is stopped until both Eq. (11) and Eq. (12) are satisfied. For any heater module, once the thermal load is known, the temperature at the outlet of the heater module can be determined.

4.2. The coupling between sCO₂ cycle and components

The partial load operation is fulfilled by adjusting the cycling mass flow rate of sCO_2 (m_{CO2}). There is an inventory tank between the state points of 8 and 2 (see Fig. 1). Adjusting m_{CO2} charges the CO_2 mass into the tank or discharges the sCO_2 mass out of the tank. Thus, the partial load operation characteristics needs to determine the cycle performance at varied mass flow rate of CO_2 . The cycle contains heat transfer components including boiler, cooler, recuperators and energy conversion components including compressors and turbines. The boiler model was described in Section 4.1. The model of recuperators can be found in Ref. [33]. We present the models for compressors and turbines.

The sCO_2 turbine operates at a relatively low pressure ratio. sCO_2 in the turbine behaves almost like an ideal gas [35,36]. Thus, the Stodola ellipse method, a classical off-design model for axial turbines, can be used for the off-design calculation of the turbine [33,35,36]. The inlet pressure of the axial turbine is predicted by the Stodola ellipse method [35,36].

$$P_{\rm in,PLO} = \sqrt{m_{\rm in,PLO}^2 T_{\rm in,PLO} Y_{\rm R} + P_{\rm out,PLO}^2}$$
 (14)

$$Y_{\rm R} = \frac{P_{\rm in,R}^2 - P_{\rm out,R}^2}{P_{\rm in,R}^2 \varphi_{\rm R}^2}, \varphi_{\rm R} = m_{\rm in,R} \frac{\sqrt{T_{\rm in,R}}}{P_{\rm in,R}}$$
(15)

where $m_{\rm in}$ is the mass flow rate entering the turbine, which equals to $m_{\rm CO2}$, P is the pressure, the subscripts of in and out refer to the inlet condition and the outlet condition respectively. The relationship of turbine efficiencies $\eta_{\rm T}$ between the rated condition and the PLO condition is [37].

$$\eta_{\text{T,PLO}} = \eta_{\text{T,R}} - 2 \cdot \left(\frac{N_{\text{PLO}}}{N_{\text{R}}} \cdot \sqrt{\frac{\Delta H_{\text{s,R}}}{\Delta H_{\text{s,PLO}}}} - 1 \right)^2$$
 (16)

where N is the rotating speed of the turbine, ΔH is the enthalpy drop

across the turbine inlet and outlet. The subscript s stands for the isentropic expansion. To keep the stable operation of the power plant, $N_{\rm PLO}$

For the sCO_2 compressors, consistent with references [9–11,15], we set the rated efficiency of compressors at 89 %. The main reasons affecting the partial load operation characteristics of the sCO₂ cycle are the reduction in main gas pressure and the relative decrease in turbomachinery mechanical efficiency [33]. Therefore, the setting of the compressor rated efficiency does not affect the results of this paper. We will conduct more detailed calculations of the compressor's rated efficiency in future research. The performance curve of the sCO2 compressor comes from Ref. [38], which is further modified by the ideal gas approach with compressibility correction (IGZ) [39], yielding the mass flow rate, enthalpy rise, rotating speed and efficiency at the PLO condition related to the rated condition as

$$m_{\rm re} = \left(\frac{m\sqrt{\gamma RZT}}{\gamma P}\right)_{\rm PLO} / \left(\frac{m\sqrt{\gamma RZT}}{\gamma P}\right)_{\rm R} \tag{17}$$

$$\Delta H_{\rm re} = \left(\frac{\Delta H}{\gamma RZT}\right)_{\rm PLO} / \left(\frac{\Delta H}{\gamma RZT}\right)_{\rm R} \tag{18}$$

$$N_{\rm re} = \left(\frac{N}{\sqrt{\gamma RZT}}\right)_{\rm PLO} / \left(\frac{N}{\sqrt{\gamma RZT}}\right)_{\rm R} \tag{19}$$

$$\eta_{\rm C,re} = \eta_{\rm C,PLO} / \eta_{\rm C,R} \tag{20}$$

where γ is the specific heat ratio, R is the universal gas constant, Z is the compression factor, the subscript re means the relative value.

Via the coupling of the cycle and the components, the parameters of sCO2 at various state points are known. Thus, the heat input per unit mass flow rate of CO_2 , q_{in} , is

$$q_{\rm in} = (1 - x_{\rm H \ 4a})(H_5 - H_4) + x_{\rm H \ 4a}(H_5 - H_{4b}) + (H_{5'} - H_{4'}) - x_{\rm EAP}(H_6 - H_{6b})$$
 (21)

The specific net work w_{net} is

$$w_{\text{net}} = (w_{\text{T1}} + w_{\text{T1}}) - (w_{\text{C1}} + w_{\text{C2}})$$

$$= (H_5 - H_{4'} + H_{5'} - H_6) - [(1 - x_{\text{C2}})(H_2 - H_1) + x_{\text{C2}}(H_{3b} - H_8)]$$
(22)

The thermal efficiency of the system is

$$\eta_{\rm th} = \frac{w_{\rm net}}{q_{\rm in}} \tag{23}$$

where $x_{\rm H4a}$ and $x_{\rm EAP}$ are the flow rate ratio entering H4a and EAP divided by the total value, H denotes the enthalpy of CO₂, the subscripts such as 4, 4', 5, 5', 6 and 6b refer to the state points (see Fig. 1).

4.3. Numerical simulation of the system performance under partial load operation conditions

The following assumptions were made under PLO conditions.

- ✓ Turbines operate at a constant speed to ensuring a 50 Hz frequency of the generated electricity.
- ✓ Compressors operate at variable speeds to maximize their efficiencies [40].
- ✓ The primary vapor temperature T_5 is constant by adjusting the coal consumption rate and the mass flow rate of CO₂ [35,41].
- ✓ The cooler provides enough cooling to sustain constant parameters of the compressor C1 [5].

The numerical simulation involves two levels of iterations. The first level is to determine the cycling mass flow rate of CO₂, which should be adapted to the net power output under PLO condition. The second level is to finalize the boiler pressure drop and the reheating temperature T_{5} ,

reflecting the coupling between the sCO₂ cycle and the components (see Fig. 6). The computational process is summarized as follows.

- ✓ Giving η_{LD} , P_1 , T_1 , T_5 and x, where x is the split ratio of mass flow
- ✓ Assuming $T_{5'}^*$ and $\Delta P_{\text{heater 1}}^*$ and $\Delta P_{\text{heater 2}}^*$. ✓ Assuming m_{CO2}^* , PLO = $m_{\text{CO2},\text{R}}\eta_{\text{LD}}$.
- ✓ Calling the subroutines of turbines, compressors, recuperators and cooler to achieve the parameters of various state points.
- ✓ Calculating $w_{\text{net,PLO}}$ and determining $m_{\text{CO2,PLO}} = \frac{W_{\text{net,PLO}}}{W_{\text{net,PLO}}}$
- ✓ The calculation of the CO₂ cycle is completed if $|m_{\text{CO2-PLO}}^*|$ $-m_{\rm CO2,PLO}$ ≤ 1 is satisfied. Otherwise, replacing $m_{\rm CO2,PLO}^*$ with $m_{\rm CO2,PLO}$ by iteration.
- ✓ Calculating $\eta_{\text{th,PLO}}$ from the parameters of various state points.
- ✓ Calculating the heat load of boiler by $Q_{\text{boiler,PLO}} = \frac{\eta_{\text{LD}} W_{\text{net,R}}}{\eta_{\text{th,PLO}}}$.
- ✓ Calculating the boiler efficiency $\eta_{\rm b,PLO}$ and determine the coal consumption rate $m_{\text{coal},PLO}$.
- ✓ Calculating the heat load and pressure drop of heater modules in the
- ✓ Achieving the boiler pressure drops of $\Delta P_{\text{heater 1}}$, $\Delta P_{\text{heater 2}}$ and the reheating temperature T_{5} . Calculating $\varepsilon_{P} = \max(|\Delta P_{\text{heater 1}}^*|$ $-\Delta P_{\mathrm{heater \ 1}}|, |\Delta P_{\mathrm{heater \ 2}}^* - \Delta P_{\mathrm{heater \ 2}}|$ and $\varepsilon_T = |T_{5'}^* - T_{5'}|$.
- ✓ Repeating the iterative process until $\varepsilon_T \le 1$ and $\varepsilon_P \le 0.001$ are satisfied.

The sCO₂ coal-fired power generation system is an emerging technology. Currently, no available experimental data on sCO2 coal-fired power generation system has been reported. The heat load of sCO₂ boiler is mainly affected by the combustion side [22], which is similar to that of water-steam boiler. Moreover, the dimensions of a sCO2 boiler and a water-steam boiler is similar. And the heat flux in furnace *q* is not sensitive to the change of the cooling wall temperature [22]. Therefore, in the absence of experimental data for sCO2 boiler, it is relatively reasonable to use the water-steam boiler heat flux curve for calculation [22]. Which is also used in the literature [22,23]. As shown in Table 5, a 600 MW supercritical steam boiler is used for the validation of the boiler thermal calculation model [42]. Under the same conditions, the deviation of the thermal calculation model in this paper is within the allowable range. This proves the accuracy of the boiler heat load calculation in this paper. Of course, CFD simulations can also be used to perform more precise calculations of the combustion heat transfer in sCO2 boilers, which we will conduct in our future work. In addition, we note that the numerical model presented in this paper is suitable not only for the rated condition, but also for the PLO condition. As shown in Table 6, our partial load model predictions well matched the results for the rated condition calculated by design model [33].

5. Results and discussion

5.1. Reheating temperatures without regulation

Fig. 7 shows the outcomes for the reheater modules in the convection region without regulation methods. Under PLO conditions, the primary vapor temperature T_5 is stabilized as 620 °C by matching the coal consumption rate and the mass flow rate of CO₂. The reheating temperature T_{5} continuously decreases as the load ratios decrease, whose deviation from the rated value reaches 32.1 °C at the load ratio of 20 % (see Fig. 7a). For the water-steam boiler, the deviation of the reheating temperature must be smaller than 10 K, which is a criterion for the partial load operation [24]. Based on this criterion, the partial load operation covers a narrow load ratio range of (80-100)%, which is not sufficient to balance the unstable renewable energies. The reheater load contribution to the total load (Q_{RH}/Q_H) is plotted in Fig. 7b, showing

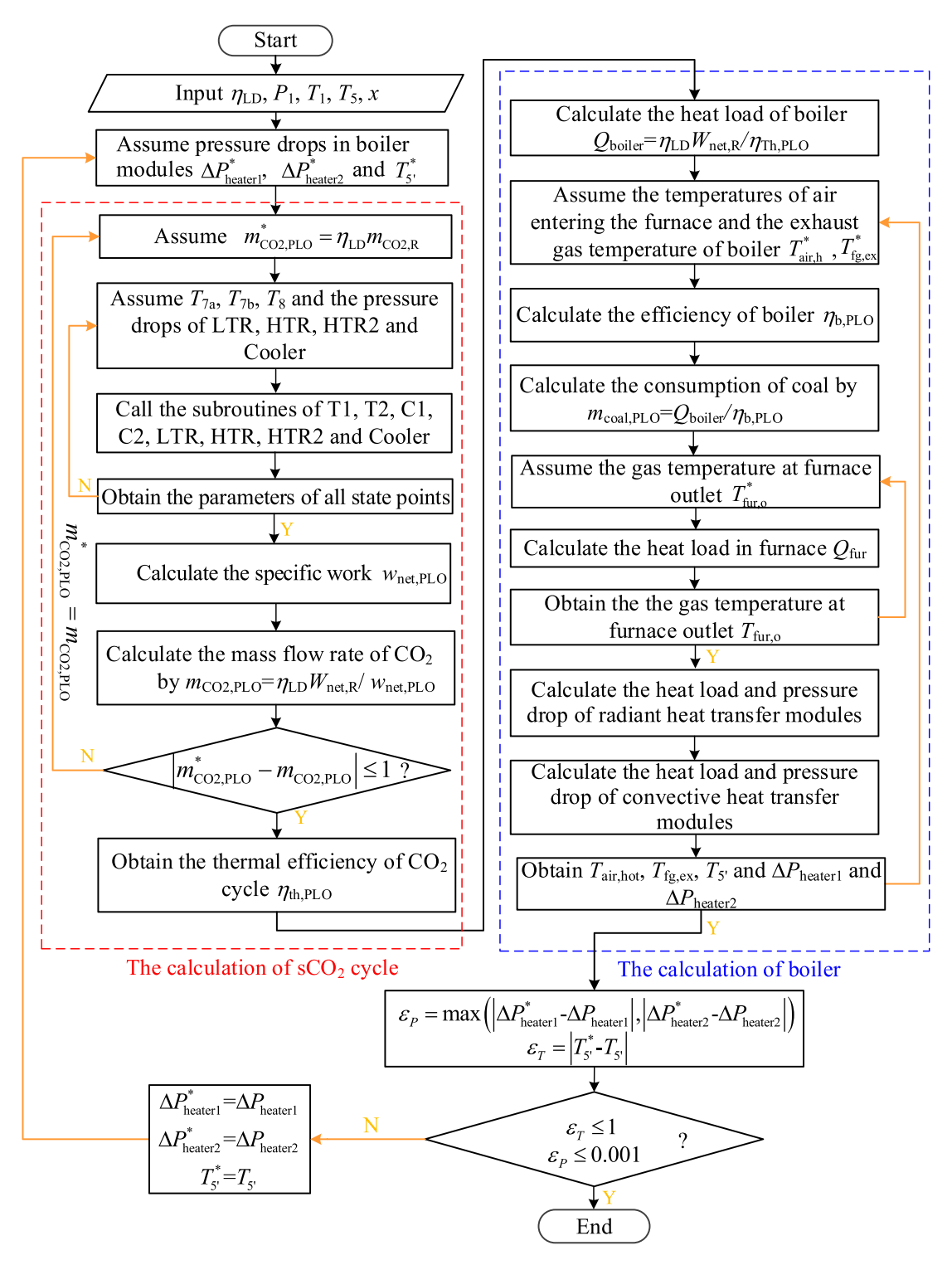


Fig. 6. The coupling between sCO_2 cycle and components under partial load operation.

obvious decrease trend as the load ratio decreases, explaining the decreased reheating temperatures shown in Fig. 7a. If one assumes constant T_5 versus load ratios, the reheater load contribution should be slightly increased as the load ratio decreases.

Fig. 7c identifies the heat absorption ratio of radiation heat transfer, illustrating the rise trend when the load ratios decrease. This is mainly because, the system uses less coal with the load ratio decreases, which lowers the mass flow rate of flue gas and lengthens the flame's residence time in furnace. This leads to a more adequate radiation heat transfer process. For the convection heating surface in boiler, the temperature at

furnace outlet decreases due to the more adequate heat exchange in furnace, lowering the heat exchange temperature difference. Additionally, the drop of coal consumption and mass flow rate of CO_2 reduce the heat transfer coefficient of convective heat transfer. Consequently, the heat absorption ratio of radiation heat transfer increases as the load ratio decreases. The variation trend of reheating temperatures without regulation under partial load operation conditions is similar to that for the water-steam boiler [25]. Fig. 7 illustrates the necessity of using the regulation methods to control the reheating temperatures.

Fig. 8 shows the T-Q diagram of the sCO₂ boiler using RCH under

Table 5Comparison of boiler design values between literature and simulation results.

Items	Literature values [42]	Simulation values	Error	Relative error (%)
T _{fur,o} (°C)	1191	1220	30	2.5
Area of superheater (m ²)	11037	11348	311	2.8
Area of re-heater (m ²)	19194.7	19928	734.3	3.8
Area of the economizer (m ²)	12974.3	13739.3	765	5.8
Area of the AP (m ²)	157800	15711	-699	-0.5

Table 6Comparison of partial load model with design model.

State	Pressure/	MPa		Temperat	ure/ºC	
points	design model	partial load model	error	design model	Partial load model	error
1	7.6	7.6	_	32.0	32.0	
2	31.20	31.21	0.01	82.5	82.5	0.01
3	31.12	31.13	0.01	232.1	232.2	0.07
4	30.95	30.95	0.01	504.8	504.4	-0.43
4b	30.11	30.11	0.01	352.0	352.0	0.03
5	30.00	30.00	-	620.0	620.0	-
4'	15.77	15.77	0.01	533.7	533.6	-0.02
5'	15.69	15.68	-0.01	620.0	620.4	0.44
6	8.20	8.20	0.01	535.5	535.0	0.42
6b	8.15	8.15	0.01	453.2	453.3	0.07
7	8.00	8.00	0.01	242.1	242.2	0.09
8	7.80	7.80	0.01	92.5	92.5	0.01

rated load (100 % load) and 50 % load conditions. Under rated load, the total thermal load of the boiler is 685 MW. At 50 % load, the total thermal load of the boiler is 371 MW. As the load ratio decreases, the inlet temperatures of the heating surfaces increase. At the same time, the exhaust temperature also decreases, which is favorable to increase the boiler efficiency.

5.2. The outcomes of RCRH method to mitigate the reheating temperatures

Perfect outcomes were achieved by using RCRH (see Fig. 9a). Covering the wide range of load ratios between 20 % and 100 %, a very gentle oscillation of reheating temperatures is observed. However, they are oscillating against the rated value of 620 °C. The difference of maximum and minimum T_5 · is only 3.5 °C, which is very favorable for the sCO₂ power plant as an adjustable energy source to balance unstable renewable energies.

We decouple the reheating load $Q_{\rm RH}$ into two parts, with one part of $Q_{\rm Part3+Part4}$ in the radiation region, and the other part of $Q_{\rm RH1+RH2}$ in the convection region (see Fig. 9b). Because the partial load operation not only decreases the radiation load in the furnace, characterized by the furnace temperature, but also decreases the flow rate of flue gas in the horizontal flue and tail flue, both $Q_{\rm Part3+Part4}$ and $Q_{\rm RH1+RH2}$ decrease when the load ratio decreases. Hence, the ratio of the reheating load $Q_{\rm RH}$ over the total load $Q_{\rm H}$ slightly increases but covers a narrow range from 38.4 % at the load ratio of 100 %–40.2 % at the load ratio of 20 % (see Fig. 9c). The variation trend of reheating loads versus load ratios using RCRH is inverse to that using the conventional arrangement shown in Fig. 7b, explaining the stabilized reheating temperatures by RCRH at different load ratios.

For the boiler using RCRH, more modules are arranged in the furnace. Therefore, at the same load ratio, the total heat load in the furnace of boiler using RCRH is higher than that of the boiler using CRH. As shown in Fig. 10, the heat load in the furnace of the boiler using

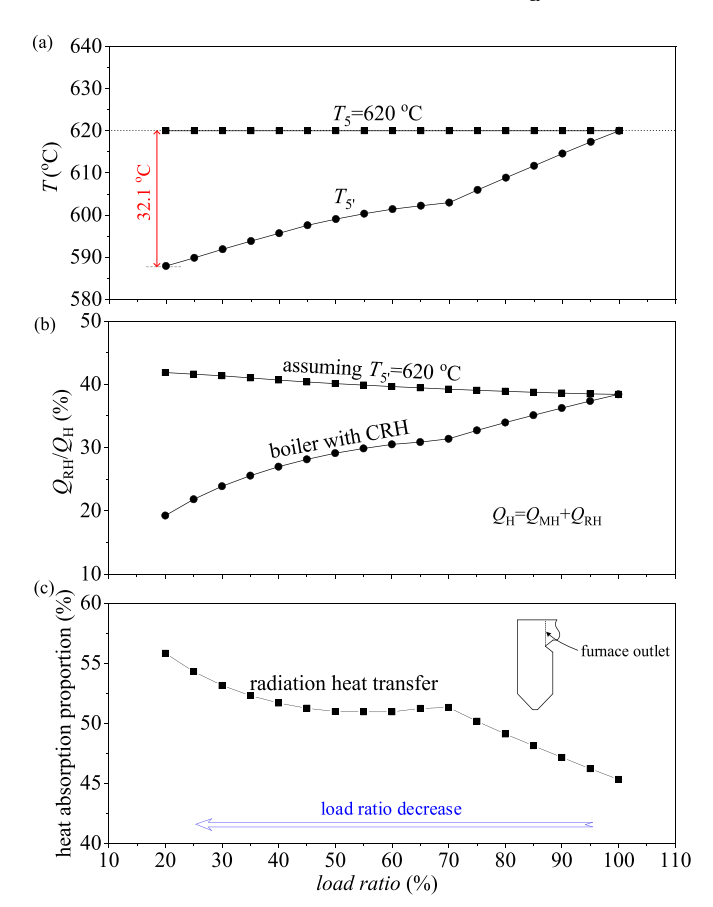


Fig. 7. Primary vapor temperature and reheating temperature under partial load operations without regulation (a: T_5 and T_5 , b: heat absorption ratio of reheater, c: heat transfer contributions of radiation).

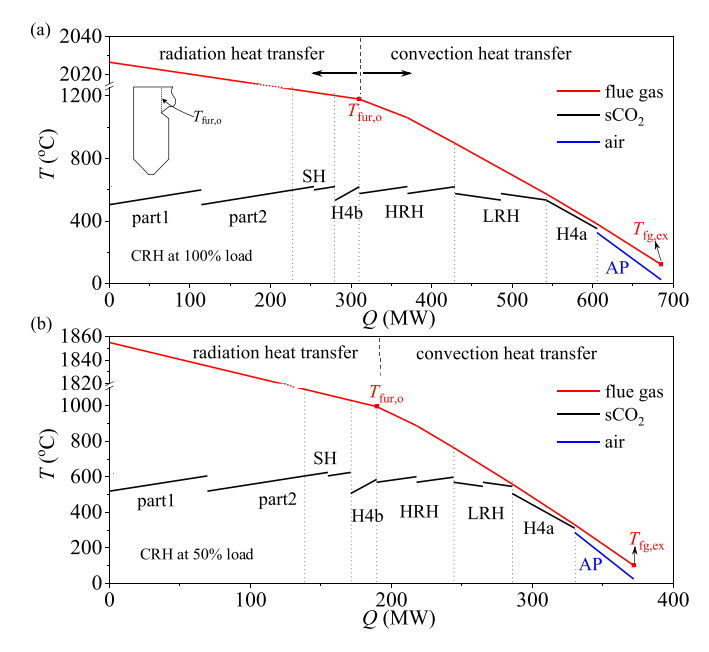


Fig. 8. T-Q curve of sCO $_2$ boiler with CRH at different load ratio (a: 100 % load ratio; b: 50 % load ratio).

RCRH is 354 MW at rated conditions, which is greater than 301 MW in the boiler using RCH (see Fig. 8a). At 50 % load, the reheat temperature of the boiler using RCRH is higher than that of the CRH boiler, making the inlet temperatures of boiler (inlets of Part1 and Part2) higher than

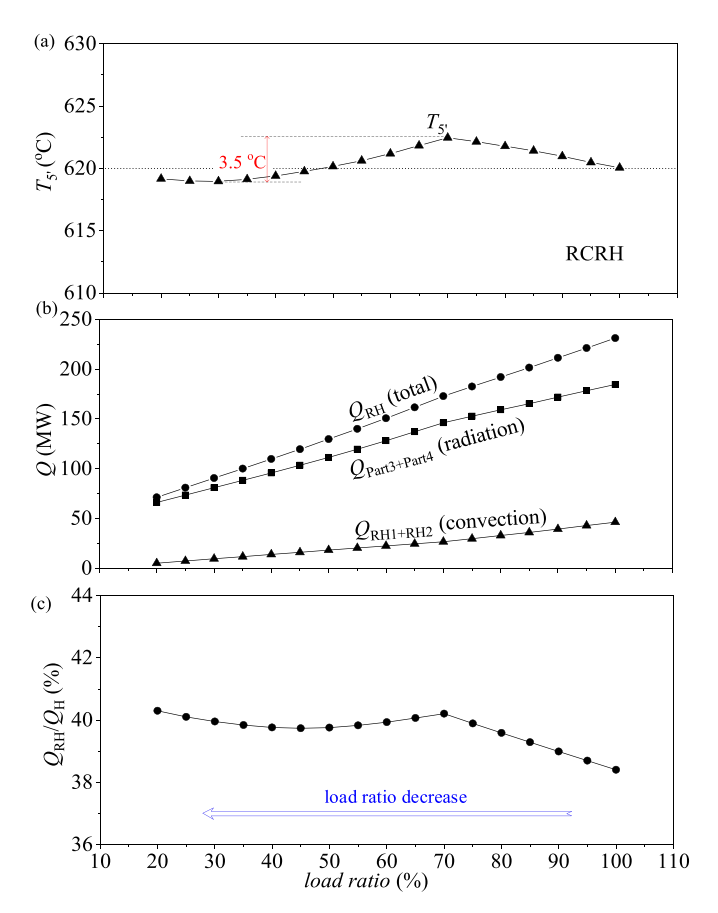


Fig. 9. Reheating temperature and reheating load contribution versus load ratios (a) reheating temperatures, b: reheating loads, c: reheating load ratio with respect to total load).

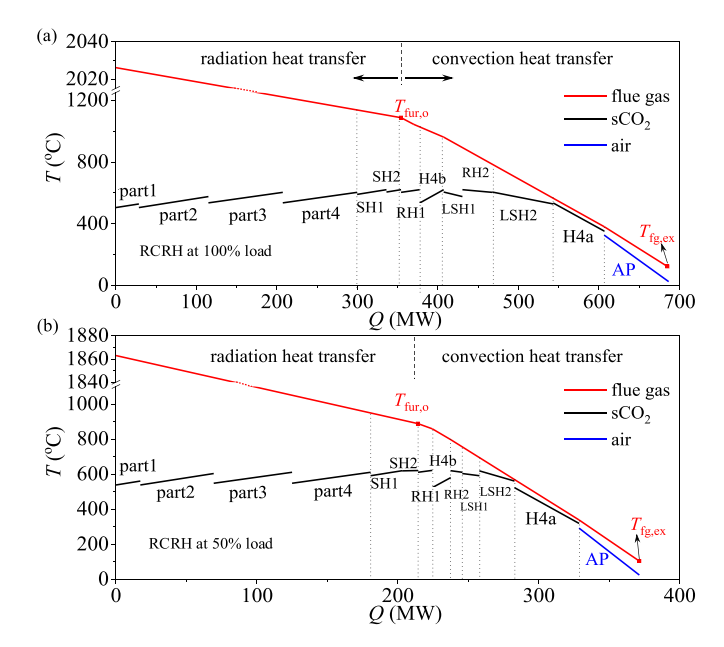


Fig. 10. T-Q curve of sCO $_2$ boiler with RCRH at different load ratio (a: 100 % load ratio; b: 50 % load ratio).

that of the boiler suing CRH (see Fig. 8b).

5.2.1. The effect of RCRH on the system performance

The effect of RCRH on the system performance was explored. Thermal efficiencies decrease with the decrease of load ratios, explained by the decreased pressure ratio and the efficiencies of compressors and turbines under PLO conditions (see Fig. 11a). This trend matches the observations in Ref. [33]. Boiler efficiency η_b characterizes the ratio of energy loss over the total chemical energy of coal during the combustion process. It is interesting to observe the parabolic distribution of boiler efficiencies against the load ratios, which is explained here. The boiler efficiency is mainly governed by the two factors, one is the flue gas temperature emitted to the environment ($T_{\rm fg,ex}$), and the other is the excess air coefficient (α). For the load ratios decreased from 100 % to 70 %, α is not changed, but the decreased $T_{\rm fg,ex}$ increases the boiler efficiencies to reach the maximum value at the load ratio of 70 %. However, for the load ratios from 70 % to 20 %, α increases to increase the flow rate to flue gas. The rise of the heat loss due to flue gas exhaust decreases the boiler efficiency.

Fig. 11b summarizes the benefit by using RCRH compared with the whole reheater modules in the convection region (CRH). Because RCRH elevates the reheating temperature to raise the turbine efficiency of T2 (see Fig. 1), RCRH has higher cycle efficiency to decrease the coal consumption rate. For example, at the minimum load ratio of 20 %, the coal consumption rate is 441.61 g/kWh with RCRH, which is lower than the value of 447.13 g/kWh with CRH.

RCRH also mitigates the flame temperature in the furnace and the flue gas temperatures in the horizontal flue. The flue gas temperature at the furnace outlet reaches 1180.2 $^{\circ}\text{C}$ with CRH, approaching the softening temperature 1190 $^{\circ}\text{C}$ of the coal, under which the furnace wall has the coking risk (see Fig. 11c). On the contrary, such flue gas temperature is 1087.4 $^{\circ}\text{C}$ with RCRH, which is far below the softening temperature of the coal, eliminating the coking risk. The reduced temperature in the furnace is benefit to improve the heat transfer performance of the cooling walls of the boiler. In summary, RCRH not only maintains suitable reheating temperature, but also ensures the safe operation of the boiler.

The cooling wall temperature is very important for the safety of the sCO_2 boiler. Excessive wall temperature can pose a risk of rupture to the pipes of heating surfaces. As shown in Fig. 12a, when the boiler uses

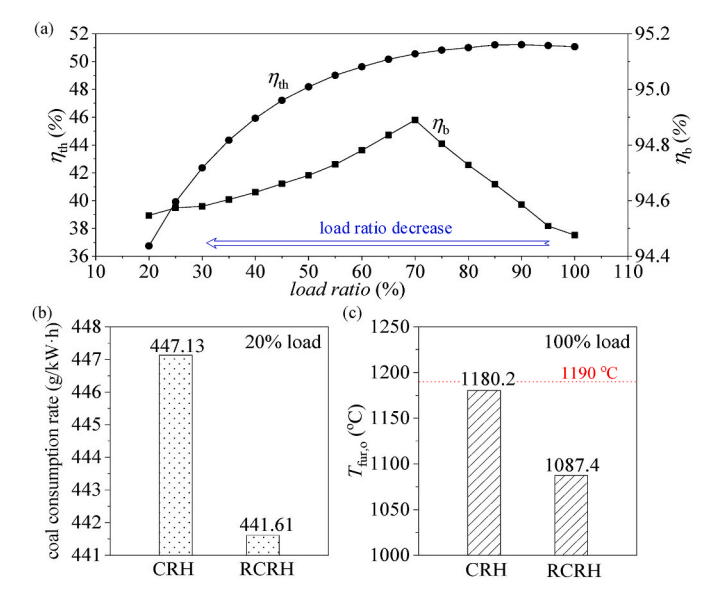


Fig. 11. The performance of the sCO₂ cycle (a: thermal efficiency and boiler efficiency using the RCRH method, b: coal consumption rate using conventional reheater (CRH) and RCRH, c: flue gas temperature at the furnace outlet using conventional reheater (CRH) and RCRH).

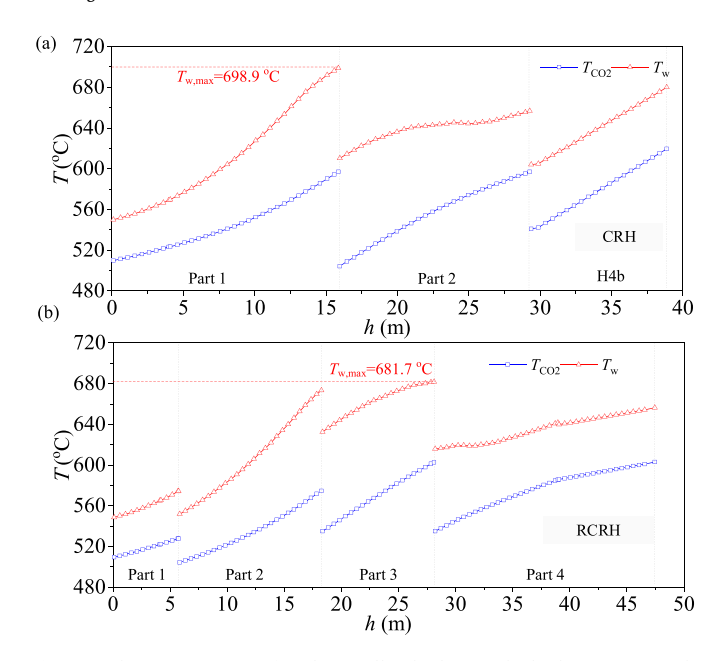


Fig. 12. The temperatures of cooling wall in boiler (a: The boiler using CRH; b: The boiler using RCRH).

CRH, the maximum wall temperature $T_{\rm w,max}=698.9~{\rm ^{\circ}C}$ occurs at the outlet of Part 1.When the boiler uses RCRH, the cooling wall is divided into more modules, which helps to reduce the temperature of the cooling wall. As shown in Fig. 12b, when using RCRH, the maximum cooling wall temperature $T_{\rm w,max}=681.7~{\rm ^{\circ}C}$ is 17.2 ${\rm ^{\circ}C}$ lower than that of RCH, occurring at the Part 3 outlet. This indicates that when using RCRH, the heating surfaces of the sCO₂ boiler has higher safety.

5.3. The outcomes of FGR method to mitigate the reheating temperatures

Here, we comment on the outcomes by using FGR for sCO_2 boilers. Apparently, FGR decreases the flame temperature in the furnace. An example case is shown at the rated condition. The flame temperature decreases from 2026.5 °C without flue gas recirculation ($r_{FGR} = 0$) to 1694.7 °C at $r_{FGR} = 30$ % (see Fig. 13a). This characteristic is similar to that for the water-steam boiler [28]. The effect of FGR on reheating temperatures T_{5} is shown in Fig. 13b, with the rise trend of reheating temperatures by using FGR covering the whole range of load ratios.

An issue occurs by using FGR. Because the load ratio of 100 % is set as the rated condition with 620 $^{\circ}\text{C}$ reheating temperature, FGR elevates the reheating temperature at high load ratios. For example, the reheating temperature becomes 635.4 °C with $r_{\rm FGR} = 30$ % at the load ratio of 100 %, which is 15.4 °C higher than the design value of 620 °C (see Fig. 13b). Thus, the vapor temperature entering the turbine T2 is obviously higher than that entering the turbine T1 inlet, which should be avoided practically. In order to overcome this issue, a hybrid FGR method is proposed, dividing the whole range of load ratios into two domains (see Fig. 13c). At high load ratios r_{FGR} is weakly mitigated, but at low load ratios it is regularly applied. The interface between the two domains is set at the load ratio of 70 %. r_{FGR} has a minimum variation with the load ratio range of (70-100) %, but is kept as 30 % with the load ratio range of (20-70) %. Even though the above effort is performed, the reheating temperature is below the designed value at low load ratios. For example, at the lowest load ratio of 20 %, the reheating temperature is 23 K below the design value, exceeding the criterion of 10 K [24], which is not acceptable for practical operation. On the other hand, if the deviation criterion of 10 K should be satisfied, the range of load ratios should cover the range of (45-100) %. In other words, FGR covers a narrow range of load ratios, corresponding to a low peak regulation

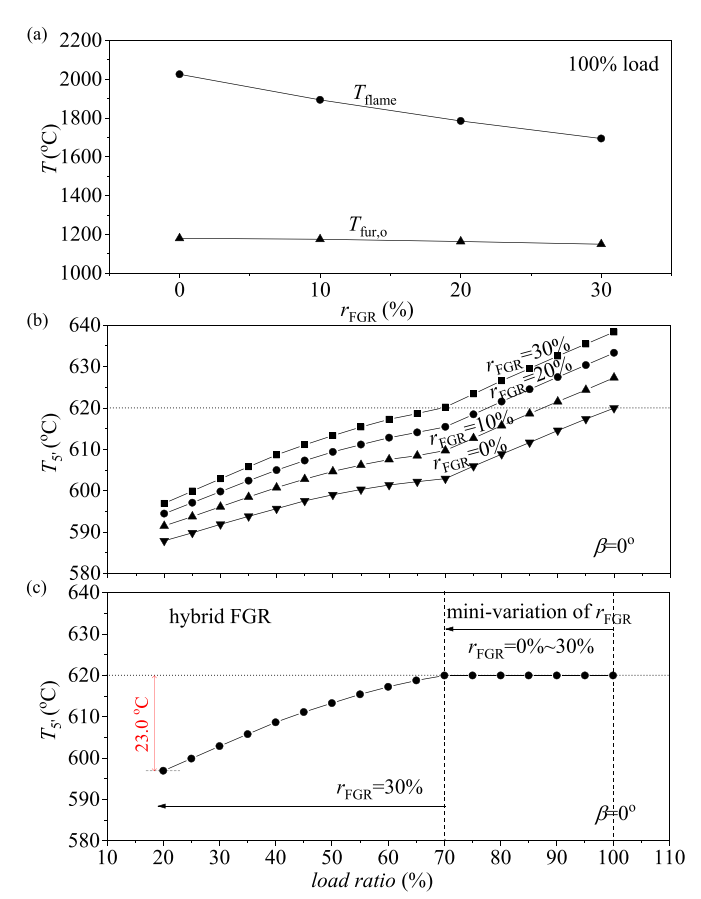


Fig. 13. Effect of FGR on flame temperatures and reheating temperatures (a: flame temperature in the furnace and flue gas temperature at the furnace outlet, b: reheating temperatures with different FGR, c: the hybrid FGR method to mitigate reheating temperatures).

depth of 55 % rated power, which is not perfect to balance the unstable renewable energies.

5.4. The BAA method to regulate the reheating temperatures

The burner angle does not change flame temperature ($T_{\rm flame}$) in the furnace, but the rise of burner angles increases flue gas temperature (Tfur,o) at the furnace outlet (see Fig. 14a), noting that positive and negative angles refer to upward inclination and downward inclination of the flame center with respect to the horizontal plane, respectively. Because negative β decreases $T_{\text{fur,o}}$ to further deteriorate the reheating temperature, the outcomes are only plotted with positive β in Fig. 14b. The reheating temperatures decrease with decrease of load ratios. The rise of burner angles elevates the reheating temperature level at low load ratios, but makes the reheating temperature exceeding the design value of 620 °C at high load ratios, which is similar to the flue gas recirculation effect illustrated in Fig. 13b. To take account of the lowest load ratio limit and the highest load ratio limit, the reheating temperatures are plotted in Fig. 14c using the hybrid BAA method. With load ratios in the range of (75-100) %, mini adjustment of burner angles is enough to stabilize the reheating temperatures. On the contrary, with the load ratios in the range of (20-75) %, the burner angle of 30° is used, which is the maximum value that can be adjusted practically. Even though the 30° angle is used, the reheating temperature is still 22 K below the design value at the load ratio of 20 %. Holding the 10 K criterion for the deviation temperatures, the power plant can only operate with the load ratios in the range of (45-100) %, not satisfying the peak regulation target.

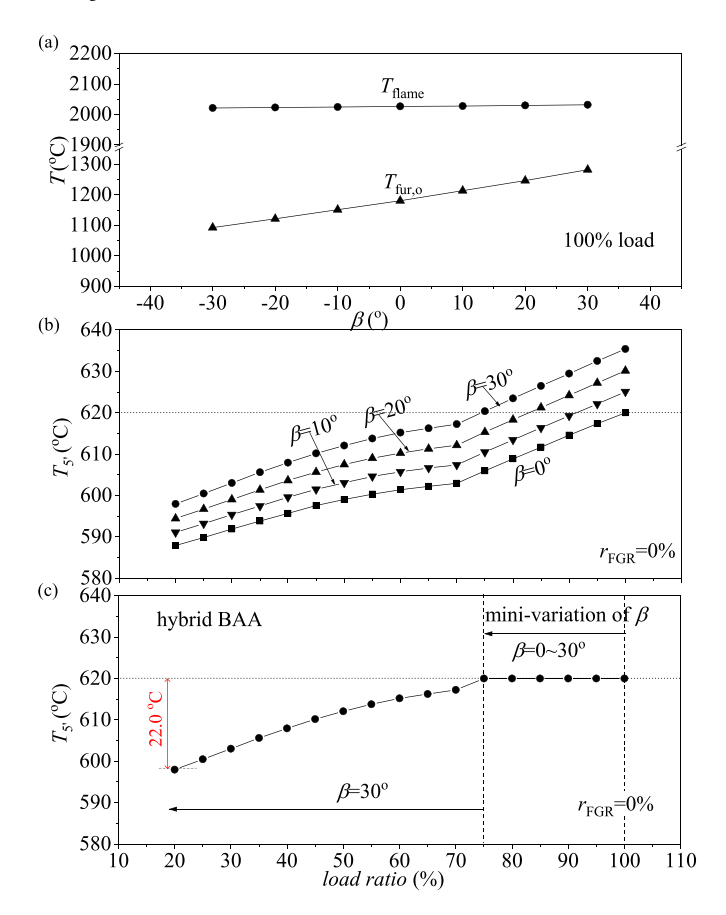


Fig. 14. Effect of BAA on flame temperatures and reheating temperatures (a: flame temperature in the furnace and flue gas temperature at the furnace outlet, b: reheating temperatures with different BAA, c: the hybrid BAA method to mitigate reheating temperatures).

5.5. Summary of comparisons between different methods

Fig. 15a summarizes the reheating temperatures mitigated by RCRH, FGR, BAA and CRH, among which RCRH and CRH are the hardware arrangement which do not depend on control system, FGR and BAA are the operation adjustment dependent on control system to activate. RCRH is perfect to mitigate the reheating temperatures. Covering the wide range of load ratios from 20 % to 100 %, the reheating temperatures are fluctuating against the rated value with the oscillating amplitude (defined as maximum subtracting minimum) of 3.5 K. The deviation between the reheating temperature from the rated value is only (1~2.5) K, not only ensuring higher cycle efficiency, but also eliminating thermal stress during partial load operations. CRH cannot adapt to the partial load operation, due to the fact that the reheating temperature sharply falls down once load ratio begins to decrease from 100 %.

FGR and BAA ensure the power plant to operate at high load ratios with reheating temperatures stabilized at the rated value of 620 °C, corresponding to the load ratio range of (75–100) % for FGR and (70–100) % for BAA. Reheating temperatures decrease beyond the high load ratio range. To satisfy the 10 K deviation criterion, both FGR and BAA cover the load ratios in the range of (45–100) %. The minimum load ratio characterizes the smallest power capacity for the coal-fired power plant to operate, which is an important index to measure the flexibility degree of the power plant. The minimum load ratio corresponds to the maximum peak load regulation depth for fossil power plant to take in the renewable energies in the grid. RCRH keeps the minimum load ratio of 20 %. Unfortunately, FGR and BAA cover the minimum load ratio of 45 %. It is concluded that the methods successfully applied for the water-

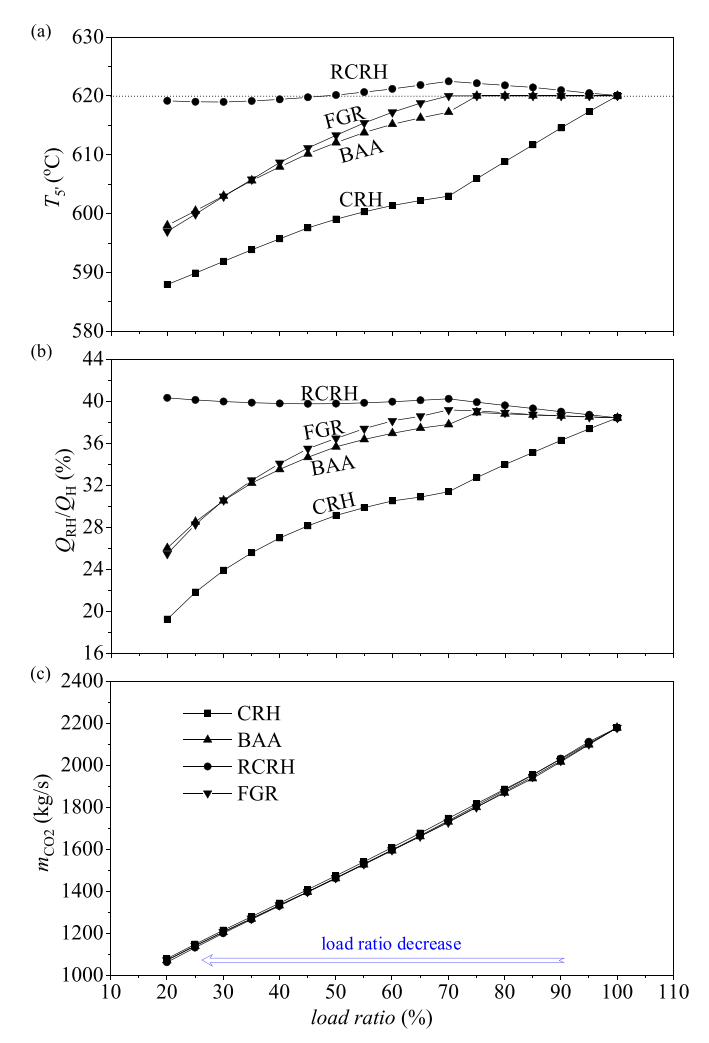


Fig. 15. Summary of different methods to regulate reheating temperatures (a: reheating temperatures T_5 ; b: reheating load ratio with respect to total load; c: mass flow rate of CO_2).

steam boiler, are not suitable for the sCO_2 boiler. The Q_{RH}/Q_H in Fig. 15b explains the data trend shown in Fig. 15a. Among the four methods, only RCRH stabilize the reheating load ratios under PLO conditions. The other three methods decrease Q_{RH}/Q_H as load ratio decreases. Fig. 15c shows the trend of CO_2 mass flow rate with load ratio under different regulation measures, it can be seen that the CO_2 mass flow rate decreases with decreasing load ratio. The effect of different regulation measures on CO_2 mass flow rate is relatively small.

Efficiency is important to determine the coal consumption rate, influencing not only the economic characteristic but also the CO2 emission. One shall pay attention to the efficiency penalty under PLO conditions. Thermal efficiency is influenced by various factors [33]. Under PLO conditions, the flow rate of CO2 of the cycle decreases to decrease the pressure drop in the boiler and the heat exchangers, which helps to stabilize the thermal efficiency. However, the decreased pressure ratio and the deteriorated efficiencies of compressors and turbines decrease the thermal efficiency of the system. The trade-off between the positive effects and negative effects decreases the thermal efficiencies as load ratios decrease (see Fig. 16a). The thermal efficiencies are weakly influenced by the reheating methods. Because the RCRH successfully stabilize the reheating temperature to improve the efficiency, which is the largest compared with other methods of FGR, CRH and BAA. At the rated condition, all the methods share the same efficiency. At the load ratio of 70 %, the thermal efficiencies are 50.56 % for RCRH, which is the largest, but becomes 50.53 % for FGR and 50.43 % for BAA. They are

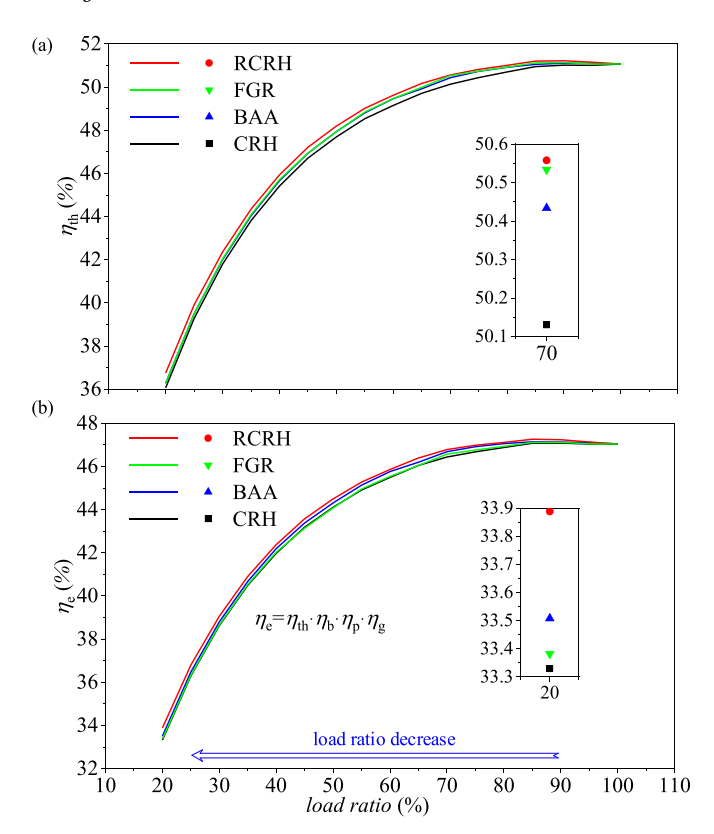


Fig. 16. Effect of different methods on efficiencies (a: thermal efficiency, b: power generation efficiency).

both larger than 50.13 % for CRH due to the increased reheating temperature.

The power generation efficiency η_e , also called the electricity efficiency, characterizes the generated electricity with respect to coal consumption, obeying $\eta_e = \eta_{\text{th}} \cdot \eta_b \cdot \eta_g \cdot \eta_p$, where η_b is the boiler efficiency (see part of the outcomes shown in Fig. 11a), η_g is the mechanical efficiency, which is set as 0.985 [33], and η_p is the pipeline efficiency, which is set as 0.99 [33]. The outcomes of electricity efficiency are shown in Fig. 16b. Under partial load operations, the system using RCRH to mitigate the reheating temperatures illustrates the largest electricity efficiency, which is 33.89 % at the load ratio of 20 %. On the contrary, the system using the conventional reheater arrangement of CRH has the efficiency of 33.33 %, which is lowest among all the mitigation methods.

It is worth noting that for the RCRH, since part of the reheater is arranged in the furnace, which limits the number of tubes in the reheater. This will increase the pressure drop of reheating process. sCO_2 coal-fired power generation system is sensitive to the reheating pressure drop [10]. Therefore, the tube diameter of the reheat heating surface must be redesigned to prevent excessive reheat pressure drop from seriously impairing thermal efficiency.

The peak shaving performance of the power generation system includes peak shaving depth and peak shaving rate. The study in this paper is to improve the reheat temperature characteristics to enable the sCO_2 coal-fired power generation system to operate over a wider load range. Which aims to improve the peaking depth of the unit. Of course, the peaking rate is also very important for the peaking performance of the unit. For example, Ref. [43] improves the variable load rate of sCO_2 coal-fired power generation system by adjusting its time constant. From the limited relevant literature, it is known that the variable load rate of sCO_2 gas-fired units is about 7.5 %Pe/min [19]. Currently, the dynamic characterization of complete sCO_2 coal-fired power generation system has not been reported. We are trying to build a dynamic model considering all the components for the sCO_2 coal-fired power generation system, focusing on its peaking rate. The related results will be reported in the future.

6. Conclusions

Both the water-steam Rankine cycle and the sCO2 cycle use the reheating technique to raise the thermal efficiency of the system. During the partial load operation, the reheating temperature shall match the primary vapor temperature to ensure the safe operation of the turbine. Usually, the reheater is located in the convection region of the boiler. As the load ratio decreases, the reheating load decreases to deteriorate the reheating temperature, which may not obey the 10 K deviation criterion from the rated value. In order to overcome this challenge, we break through the limitation of the reheater arrangement in the convection region. We smartly use the modular heater characteristic of the sCO₂ boiler, decoupling the reheater into four modules, among which two are located in the radiation region and two in the convection region. The above arrangement is called the radiation-convection-reheater (RCRH) in this paper. A boiler load assignment model is established, which is coupled with the thermodynamics analysis. The outcomes of the reheating temperatures as well as the system performance are presented for the systems using the methods of RCRH, FGR and BAA. It is found that both FGR and BAA cover narrow load ratio range of (45-100) % to satisfy the 10 K reheating temperature deviation, indicating not effectiveness of the two methods. On the contrary, RCRH mitigates the reheating temperature deviation to $(1\sim2.5)$ K covering a wide load ratio range of (20-100) %, indicating a large peak regulation depth of 80 % rated power, benefiting from the heat absorption ratio of the radiation component and the convection component synchronously varies as load ratio decrease to stabilize the reheating temperature. The proposed RCRH ensures the sCO₂ power plant to operate at an ultra-low load ratio, which can be regarded as an adjustable energy source to balance the unstable renewable energies.

Nomenclature

A	area, m ²	Greek symbols		
d	diameter, mm	α	excess air coefficient;	
Н	specific enthalpy, kJ/kg; high, m	β	burner angle	
K	the heat transfer coefficient, $W/(m^2K)$	δ	tube wall thickness	
m	mass flow rate, kg/s	ΔT	temperature difference, °C	
N	rotating speed, rpm	ΔP	pressure difference, MPa	
P	Pressure, MPa	ε	comprehensive blackness; iteration error	
q	heat loss, %; the heat load per unit mass flow rate of CO ₂ , kJ/kg	φ	boiler heat retention coefficient	
Q	thermal load, MW; heating value of coal or flue gas, kJ/kg	γ	ratio of specific heat capacity	
r	Ratio, %	η	efficiency or ratio, %	
R	gas constant, J/kgK	φ	non-uniform coefficient	
S	tube pitch, mm			
T	Temperature, °C	Abbrevo	ations	
W	output/input work, MW	AP	air preheater	
x	split ratio of flow rate	BAA	burner angle adjustment	
z	high, m	C1, C2	compressor	
Z	gas compressibility	CRH	convection reheater	
		EAP	external air preheater	
		FGR	flue gas recirculation	
Subscripts		FDA	flue gas damp adjustment	
1, 2, 3	state points of cycle	HRH	high temperature reheater	
b	boiler	HTR	high temperature regenerative heat exchanger	
C	compressor	H4a	Heater 4a	
e	electricity	H4b	Heater 4b	
ex	exhaust	IGZ	the ideal gas approach wit compressibility correction	
fg	flue gas	LSH	low temperature superheater	
			(

(continued on next page)

(continued)

fur	furnace	LTR	low temperature
			regenerative heat
			exchanger
H	heater	PLO	partial-load-operations
in	input or inlet	RC	Recompression cycle
LD	load	RCRH	Radiation-convection
			reheater
LHV	lower heating value	RH	reheater
MH	main heater	SA	spray attemperation
out	outlet	sCO_2	supercritical carbon
			dioxide
О	outlet; outer of rube	SH	superheater
R	rated conditions	SOFA	separated overfired air
RH	reheater	T1,	turbine
		T2	
re	relative	TC	tri-compression cycle
s	isentropic	V1-2	valve 1-2
th	thermal		

CRediT authorship contribution statement

Haonan Zheng: Writing - original draft, Software, Methodology, Investigation. Jinliang Xu: Writing – review & editing, Methodology, Funding acquisition, Conceptualization. Jian Xie: Methodology, Conceptualization. Guanglin Liu: Writing - review & editing, Methodology.

Declaration of competing interest

We state that the manuscript titled as "Regulation of reheating temperatures for sCO2 power plant to balance unstable renewable energies" by Haonan Zheng, Jinliang Xu, Jian Xie, Guanglin Liu does not have any conflict of interest including any financial, personal or other relationships with other people or organizations within three years of beginning the submitted work that could inappropriately influence, or be perceived to influence, the present work.

Acknowledgements

This work was supported by the Natural Science Foundation of China (51821004, 52130608).

Data availability

No data was used for the research described in the article.

References

- [1] Raza MY, Lin B. Energy transition, carbon trade and sustainable electricity generation in Pakistan. Appl Energ 2024;372:123782. https://doi.org/10.1016/j.
- [2] He Y, Qiu Y, Wang K, Yuan F, Wang W, Li M, et al. Perspective of concentrating solar power. Energy 2020;198:117373. https://doi.org/10.1016/j.
- [3] Denholm P, Cole W, Blair N. Moving Beyond 4-Hour Li-Ion Batteries: Challenges and Opportunities for Long(er)-Duration Energy Storage. Golden, CO: National Renewable Energy Laboratory. NREL/TP-6A40-85878 https://www.nrel.gov/ docs/fy23osti/85878.pdf..
- [4] Zhao Y, Wang C, Liu M, Chong D, Yan J. Improving operational flexibility by regulating extraction steam of high-pressure heaters on a 660 MW supercritical coal-fired power plant: a dynamic simulation. Appl Energ 2018;212:1295–309. https://doi.org/10.1016/j.apenergy.2018.01.017
- [5] Fan G, Dai Y. Thermo-economic optimization and part-load analysis of the combined supercritical CO2 and Kalina cycle. Energ Convers Manage 2021;245: 114572. https://doi.org/10.1016/j.enconman.2021.114572.
- [6] Ma T, Li M, Xu J, Ni J, Tao W, Wang L. Study of dynamic response characteristics of S-CO2 cycle in coal-fired power plants based on real-time micro-grid load and a novel synergistic control method with variable working conditions. Energ Convers Manage 2022;254:115264. https://doi.org/10.1016/j.enconman.2022.115264.
 [7] Liese E, Albright J, Zitney SA. Startup, shutdown, and load-following simulations of
- a 10 MWe supercritical CO2 recompression closed Brayton cycle. Appl Energ 2020; 277:115628. https://doi.org/10.1016/j.apenergy.2020.115628.

- [8] Le Moullec Y. Conceptual study of a high efficiency coal-fired power plant with CO₂ capture using a supercritical CO₂ Brayton cycle. Energy 2013;49:32-46. doi.org/10.1016/j.energy.2012.10.022
- [9] Zhou J, Ling P, Su S, Xu J, Xu K, Wang Y, et al. Exergy analysis of a 1000 MW single reheat advanced supercritical carbon dioxide coal-fired partial flow power plant. Fuel 2019;255:115777. https://doi.org/10.1016/j.fuel.2019.1157
- [10] Xu J, Sun E, Li M, Liu H, Zhu B. Key issues and solution strategies for supercritical carbon dioxide coal fired power plant. Energy 2018;157:227-46. https://doi.org/
- [11] Li H, Zhang Y, Yang Y, Han W, Yao M, Bai W, et al. Preliminary design assessment of supercritical CO2 cycle for commercial scale coal-fired power plants. Appl Therm Eng 2019;158:113785. https://doi.org/10.1016/j.
- [12] Li Z, Li Z, Li J, Feng Z. Leakage and rotordynamic characteristics for three types of annular gas seals operating in supercritical CO2 turbomachinery. J Eng Gas Turbines Power 2021;143. https://doi.org/10.1016/10.1115/1.4051104
- [13] Cui X, Guo J, Huai X, Zhang H, Cheng K, Zhou J. Numerical investigations on serpentine channel for supercritical CO2 recuperator. Energy 2019;172:517-30. loi.org/10.1016/j.energy.2019.01.14
- [14] Zhou J, Zhu M, Xu K, Su S, Tang Y, Hu S, et al. Key issues and innovative doubletangential circular boiler configurations for the 1000 MW coal-fired supercritical carbon dioxide power plant. Energy 2020;199:117474. https://doi.org/10.1016/j.
- [15] Wang Z, Zheng H, Xu J, Li M, Sun E, Guo Y, et al. The roadmap towards the efficiency limit for supercritical carbon dioxide coal fired power plant. Energ Convers Manage 2022;269:116166. https://doi.org/10.1016/j. enconman, 2022, 116166.
- [16] Fan YH, Yang DL, Tang GH, Sheng Q, Li XL. Design of S-CO2 coal-fired power system based on the multiscale analysis platform. Energy 2022;240:122482. https://doi.org/10.1016/j.energy.2021.122482.
- Alfani D, Binotti M, Macchi E, et al. sCO₂ power plants for waste heat recovery: design optimization and part-load operation strategies. Appl Energ 2021;195:
- [18] Alfani D, Astolfi M, Binotti M, et al. Part-load operation of coal fired sCO2 power plants. Proceedings of the 3rd European conference on supercritical CO2 (sCO2) power systems. 2019. p. 1-10. https://doi.org/10.17185/duepublico/48897.
- [19] Liese E, Albright J, Zitney SA. Startup, shutdown, and load-following simulations of a 10 MWe supercritical CO2 recompression closed Brayton cycle. Appl Energy
- [20] Sun E, Xu J, Li M, Liu G, Zhu B. Connected-top-bottom-cycle to cascade utilize flue gas heat for supercritical carbon dioxide coal fired power plant. Energ Convers Manage 2018;172:138–54. https://doi.org/10.1016/j.enconman.2018.07.017.
- Sun E, Xu J, Hu H, Li M, Miao Z, Yang Y, et al. Overlap energy utilization reaches maximum efficiency for S-CO2 coal fired power plant: a new principle. Energ Convers Manage 2019;195:99-113. https://doi.org/10.1016/j. enconman, 2019, 05, 009.
- [22] Liu C, Xu J, Li M, Wang Z, Xu Z, Xie J. Scale law of sCO2 coal fired power plants regarding system performance dependent on power capacities. Energ Convers Manage 2020;226:113505. https://doi.org/10.1016/j.enconman.2020.1
- [23] Li Y, Zhou L, Xu G, Fang Y, Zhao S, Yang Y. Thermodynamic analysis and optimization of a double reheat system in an ultra-supercritical power plant. Energy 2014;74:202-14. https://doi.org/10.1016/j.energy.2014.05.057
- [24] Che D, Zhuang Z, Li J, Wang D. Boilers: theory, design and operation. Xi'an, China: Xi'an Jiaotong University Press; 2008.
- [25] Bao S. Variable load calculation and sensitivity analysis of 1000MW power boiler. Beijing, China: North China Electric Power University; 2019.
- [26] Zhou Q. Boiler mechanism. Beijing, China: China Electric Power Press; 2013.
 [27] Liu H, Yu P, Xue J, Deng L, Che D. Research and application of double-reheat boiler in China. Processes 2021;9:2197. https://doi.org/10.3390/pr9122197.
- Ma K, Li CF, Yan WP, Sun JW, Cai P, Huang QL. Effect of flue gas recirculation on reheated steam temperature of a 1000MW ultra-supercritical double reheat boiler. IOP Conf Ser Earth Environ Sci 2018;146:12043. https://doi.org/10.1088/1755
- [29] Zhang G, Xu W, Wang X, Yang Y. Analysis and optimization of a coal-fired power plant under a proposed flue gas recirculation mode. Energ Convers Manage 2015; 102:161-8. https://doi.org/10.1016/j.enconman.2015.01.07
- Fan H, Xu W, Zhang J, Zhang Z. Steam temperature regulation characteristics in a flexible ultra-supercritical boiler with a double reheat cycle based on a cell model. Energy 2021;229:120701. https://doi.org/10.1016/j.energy.2021.120701.
- [31] Zhu H, Tan P, He Z, Ma L, Zhang C, Fang Q, et al. Revealing steam temperature characteristics for a double-reheat unit under coal calorific value variation. Energy 2023;283:128530. https://doi.org/10.1016/j.energy.2023.128530.
- [32] Zhu X, Wang W, Xu W. A study of the hydrodynamic characteristics of a vertical water wall in a 2953t/h ultra-supercritical pressure boiler. Int J Heat Mass Tran 2015;86:404-14. https://doi.org/10.1016/j.ijheatmasstransfer.2015.03.010.
- [33] Zheng H, Miao Z, Xu J. Partial load operation characteristics of supercritical CO2 coal-fired power generation system. Energy 2024;291:130415. https://doi.org/ 10.1016/j.energy.2024.130415
- Alfani D, Astolfi M, Binotti M, Silva P. Part Load strategy definition and annual simulation for small size sCO2 based pulverized coal power plant. In: Turbo expo: power for land, sea, and air. London, England: American Society of Mechanical Engineers; 2020.
- [35] Hu H, Liang S, Jiang Y, Guo C, Guo Y, Zhu Y, et al. Thermodynamic and exergy analysis of 2 MW S-CO2 Brayton cycle under full/partial load operating conditions. Energ Convers Manage 2020;211:112786. https://doi.org/10.1016/j

- [36] Fan G, Li H, Du Y, Chen K, Zheng S, Dai Y. Preliminary design and part-load performance analysis of a recompression supercritical carbon dioxide cycle combined with a transcritical carbon dioxide cycle. Energ Convers Manage 2020; 212:112758. https://doi.org/10.1016/j.enconman.2020.112758.
- [37] Ray A. Dynamic modelling of power plant turbines for controller design. Appl Math Model 1980;4:109–12. https://doi.org/10.1016/0307-904X(80)90114-6.
- [38] Wang Y, Guenette G, Hejzlar P, Driscoll M. Compressor design for the supercritical CO2 Brayton cycle. In: 2nd international energy conversion engineering conference; 2004. p. 5722.
- [39] Jeong Y, Son S, Cho SK, Baik S, Lee JI. A Comparison study for off-design performance prediction of a supercritical CO2 compressor with similitude analysis. In: Fluids engineering division summer meeting. American Society of Mechanical Engineers; 2019. V3A.
- [40] Dostal V, Driscoll MJ, Hejzlar P. A supercritical carbon dioxide cycle for next generation nuclear reactors. Massachusetts Institute of Technology, Department of Nuclear Engineering; 2004.
- [41] Tong Y, Duan L, Pang L. Off-design performance analysis of a new 300 MW supercritical CO2 coal-fired boiler. Energy 2021;216:119306. https://doi.org/ 10.1016/j.energy.2020.119306.
- [42] Zhi X. Design of 600 MW pulverized coal-fired boiler. Hangzhou, China: Zhejiang University; 2007.
- [43] Alfani D, Astolfi M, Binotti M, Campanari S, Casella F, Silva P. Multi objective optimization of flexible supercritical CO2 coal-fired power plants. Turbo expo: power for land, sea, and air, vol. 58608. American Society of Mechanical Engineers; 2019, V003T06A027. https://doi.org/10.1115/GT2019-91789.